A STUDY OF EXPLODING WIRES

Thesis by

Ben Robert Turner

In Partial Fulfillment of the Requirements

for the Degree of

Doctor of Philosophy

California Institute of Technology

Pasadena, California

1960

ACKNOWLEDGEMENTS

The writer wishes to express his gratitude to Professor Milton S. Plesset for suggesting this study and for his guidance, and to Professor Robert B. King for his cooperation and helpful advice. I also wish to thank Professor Albert T. Ellis for the useful suggestions and encouragement he has given in the experimental work.

Special thanks are due to Dr. Carl Rouse of the Ernest O. Lawrence Radiation Laboratory for theoretical computations which he has carried out for comparison with the experimental results.

ABSTRACT

Experimental observations were made of exploding wires of different sizes and types. Explosions in air and vacuum were studied. Kerr cell pictures were taken in air and the time dependent energy input obtained. The shock wave was photographed and compared with theoretical calculations from which estimates of other quantities were made. The time integrated spectral energy density was determined for the wave length region 2300 $\mathring{A}$ - 5500 $\mathring{A}$ for 3 mil diameter iron wire. Photographs of the exploding wires in a vacuum of 10^{-5} mm Hg are presented and discussed.

The maximum energy which could be stored was 7500 joules. Most of the experimental work was done using 3.75 microfarads charged to 40 kv with a circuit resonance frequency of 50 kc. Pictures were taken at the rate of 4×10^5 frames per second in most cases, with exposure times of about 1/20 microsecond.

TABLE OF CONTENTS

LIST OF FIGURES

I. INTRODUCTION

The study of wires exploded by means of large current pulses through them has had, so far, three distinct stages of development. The first, beginning shortly before 1800 and continuing until about 1920, was a period during which exploding wires were mentioned only occasionally. Little could be accomplished during this period because of the lack of methods of observation in the microsecond region. The second phase began with the work done by J. A. Anderson[1, 2] and lasted until the early 1950's. During this time much work was done in studying spectroscopic phenomena, and papers involving exploding wires were published frequently. During the 1950's exploding wire research was accelerated again, this time because of the fusion projects and the use of Kerr cell cameras. Several Russian publications appeared[3, 4], and research in this country on all features of the exploding wire has continued on a large scale. Sometimes exploding wires were studied because of interest in the phenomena for their own sakes and sometimes because useful applications were found.

The majority of work which has been done and is being done is experimental. There has been some theoretical progress on certain aspects of the exploding wire among which may be mentioned a similarity solution for cylindrical shock waves[5] and, more recently, Rouse[6] has undertaken a series of theoretical calculations in which the intention is to make the model for his analysis gradually more complicated, first considering the gross characteristics and later adding refinements to account for remaining effects.

Applications of the exploding wire include the production of thin films of certain metals without liquefying; a high voltage, fast response fuse; a high power pulse steepener; a short duration, high intensity light source for photographing rapid events; and many others. Wire explosions can produce high temperatures at high densities where little information now exists on the equation of state. An estimate of the temperature attainable is about 20, 000°C[1] when the explosion occurs in air and several times this figure when in a liquid.

Exploding wires may be classed according to the behavior of the current oscillogram. Under certain conditions, depending upon the parameters of the circuit and the size and type of wire, there may be a period of very low conductivity immediately after the wire has been gasified. Under this type of behavior, the current oscillogram shows an initial pulse of current followed by a period of up to about a hundred microseconds during which no current flows. Then the current begins again and follows a damped sine wave shape. This case goes smoothly into the case where the current follows a damped sine wave shape from its beginning; when the time of the "dwell" becomes zero, there is still a rapid drop followed by a sine wave rise in the current. As the conditions are further removed from those required for the dwell to occur, the amount of the drop becomes less and less until, finally, it is no longer noticeable. There are several theories of the cause of this "current pause" or "dwell" or "dark time" based on very different physical factors (compare, for example, references (3) and (6), pp. 9-11).

The objective of the present investigation has been to ascertain as much about the many characteristics of exploding wires as possible.

The work was of an exploratory nature, and much time was spent in the development of laboratory techniques. Emphasis has been placed on the reliability of the data, but an effort was also made to be as accurate as possible. Where a questionable method or assumption is involved, an attempt was made to state and discuss the problem involved. Some parts of the work reported here are amenable to much greater accuracy than others. The investigation can be divided into four major parts:

1. Observations of explosions in air with emphasis on obtaining data concerning the hydrodynamic flow,

2. Comparison of the experimental results obtained in Part II with the Rouse theory,

3. Observations of explosions in vacuum,

4. A study of the continuous radiation using a photographic method.

II. APPARATUS

The Discharge Circuit

The basic equipment used in this study of the exploding wire is summarized by the block diagram in Fig. 1. A corresponding photograph of the equipment when taking Kerr cell pictures of the wire explosions in air is shown in Fig. 2. In operation, when Kerr cell pictures were being taken, for example, the charging of C_1 was begun after the wire to be exploded had been set in place. The charging current was left on this bank so as to compensate for leakage while the operator carried out such last minute details as opening the shutter on the recording camera of the oscilloscope, bringing the turbine up to speed, and opening the Kerr cell shutter. Then the double-pole double-throw switch was thrown and bank C_2 charged. When it had completed charging, the double-pole double-throw switch was lifted to a neutral position so that the system had only one ground. The switch to the thyratron circuit in the Kerr space cell pulser was closed, simultaneously firing the spark gap switch and putting pulses on the Kerr cell so that pictures were taken of the wire explosion. The shutters of the recording camera and the Kerr cell camera were then closed, the turbine was stopped, and any remaining charge on the capacitors discharged.

To store energy, 16 Westinghouse 1.5 microfarad, 25,000 volt inerteen type FP capacitors, each having a measured inductance of .51 microhenries were employed giving a maximum total energy storage of 7500 joules. These were mounted in two groups of 5 and a remaining

group of 6. A group of 5 and a group of 6 were placed on insulators which could withstand high voltages; the remaining group of 5 was on rubber rollers, but not otherwise insulated. This type of mounting gave considerable freedom in how these capacitors were to be used. In some parts of this work all the capacitors were used. For most of the Kerr-cell photographs, the two 5 capacitor banks were used in series; each group was charged to 20 kv so that the result was 3.75 microfarads charged to 40 kv. The stored energy in this case was approximately 3000 joules. It was actually slightly less than this because the bank first charged lost some of its charge through leakage while the second bank was being charged.

For switching the discharge, a spark gap was found to be most suitable. Originally a vacuum switch was planned for this purpose. This switch was donated for this work by the Jennings Radio Manufacturing Corporation of San Jose, California. However, it was found that identical current oscillograms were obtained when either this switch or the spark gap was used. The vacuum switch had the disadvantage of being mechanical in nature so that the synchronization necessary for Kerr cell photographs of the wire was impossible. In addition, this switch could withstand only 20 kv before breaking down. To fire the spark gap a thyratron in the Kerr cell pulser discharged a 2.00 microfarad condenser charged to 600 volts through an automobile coil. There was approximately a 20 microsecond delay from the time that the thyratron broke down until the spark gap fired. This gave sufficient time for the Kerr cell to begin to function properly. A 30 kv, 500 micromicrofarad television condenser separated the spark coil

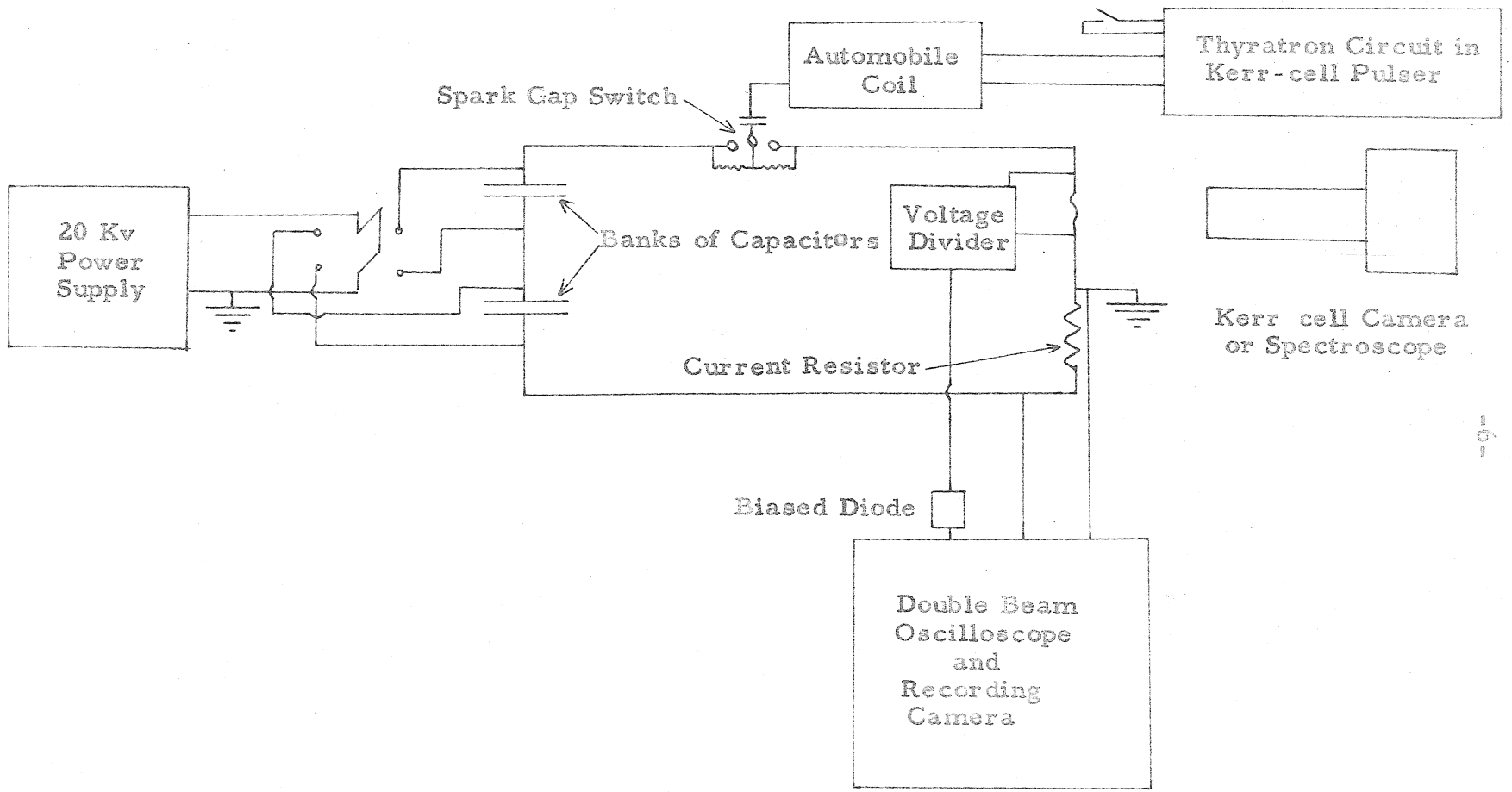

Fig. 1. Block diagram of apparatus

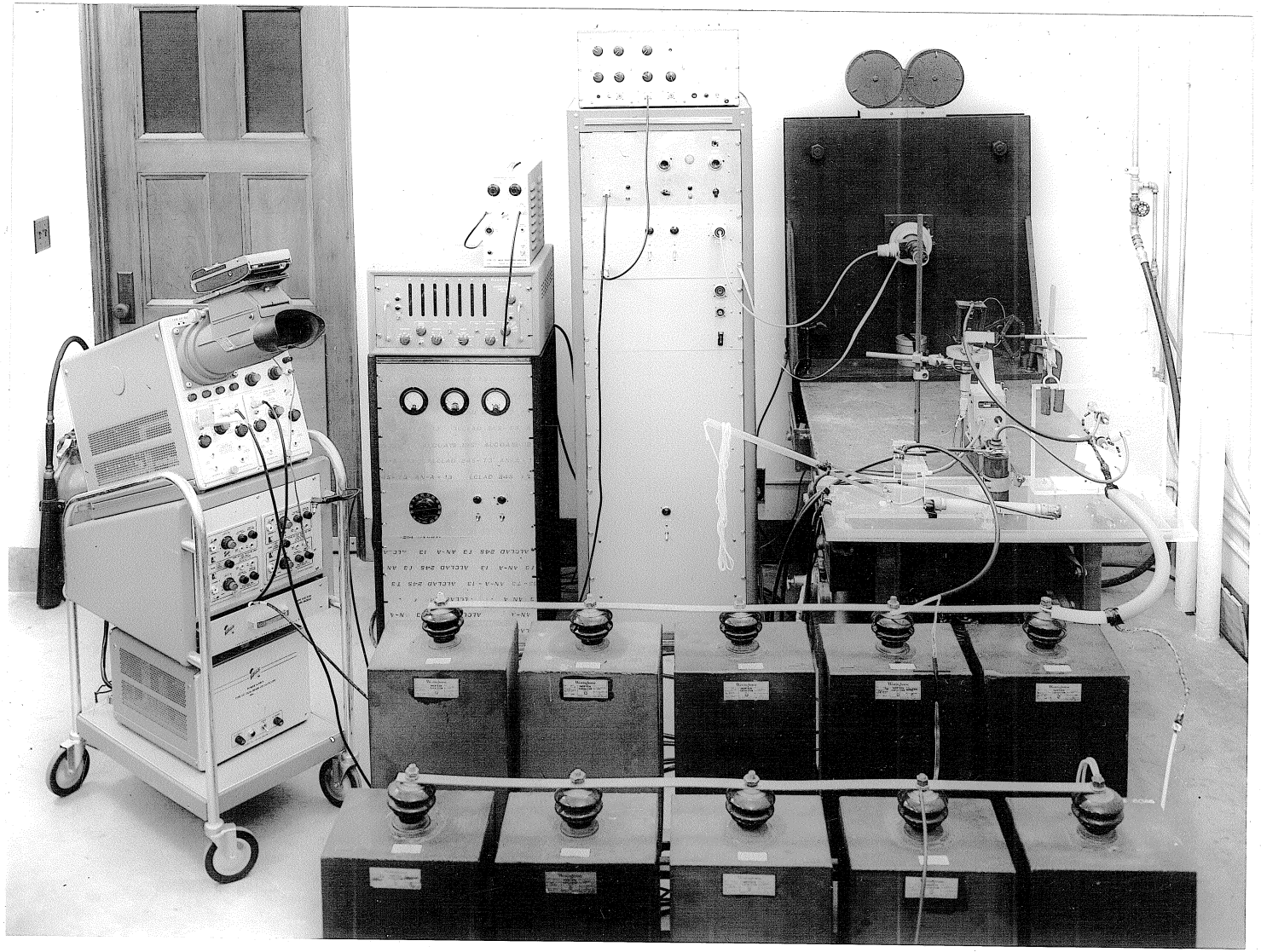

Fig. 2. Photograph of apparatus

from center knob of the spark gap to prevent the discharge from passing through the coil. The spark gap itself consisted of three brass spheres 1-1/4 inch in diameter mounted so that the distance between them could be adjusted. The potential of the center sphere was held at one-half that of the high voltage sphere by means of 9 ten megohm resistors. Without these resistors the spark gap did not break down reliably.

Current-Measuring Resistor

One of the most significant measurements made during a wire explosion was that of the current oscillogram. This measurement could be made accurately and used as a convenient method for comparing different exploding wire experiments.

The method used to obtain the current oscillogram was to measure the voltage developed across a known inductance-free resistance which was placed in series with the exploding wire. Great care had to be taken in the construction of this resistance in order to be certain that the self-inductance of the resistor made a negligible contribution to the signal. Since currents of the order of 40,000 amperes were passed through this resistor, a resistance value of .002 ohms was convenient. The frequency of this current was about 50 kc. Thus the inductance had to be less than $1/3 \times 10^{-3}$ microhenries if inductive effects contributed less than 5% of the voltage being measured. This value of inductance cannot easily be measured, and so the resistor had to be constructed in such a way that the inductance could be accurately calculated. Many types of resistors were tried, but the only one which proved satisfactory is shown in Fig. 3. This was a modification of a

design by the National Bureau of Standards. Note that the voltage was developed across two points on the same cylinder so that no soldered connection was included. All the important connections were silver soldered. It was permissible to measure the value of this resistance by a DC method for the frequency mentioned above, since skin effects did not become significant until much higher frequencies. The value of the resistance obtained by the voltmeter-ammeter method using a Hewlett Packard microvoltmeter and a Simpson meter as a milliammeter was .0019 ohms. Its inductance was calculated and was 1.67×10^{-3} microhenries, which was not quite negligible. Current oscillograms obtained with this resistor were easily corrected to account for this small inductance.

Voltage Divider

Another important electrical measurement which could be made during the wire explosion was that of the voltage oscillogram. The rate of change of current in this experiment was of the order of 10^{10} amperes/sec so that care had to be taken to insure that the induced emf developed across the measuring circuit was small compared with the voltage across the wire.

The circuit used to obtain the voltage oscillogram is shown in Fig. 4. A capacitance voltage divider was used with a resonance at approximately 30 megacycles. The time constant of the decay of these oscillations was .5 microsecond. When a square wave was applied to the voltage divider, the output signal dropped 33% in 500 microsecond. As previously mentioned, the frequency of the discharge was about 50 kilocycles and only about the first 20 microsecond were studied so that

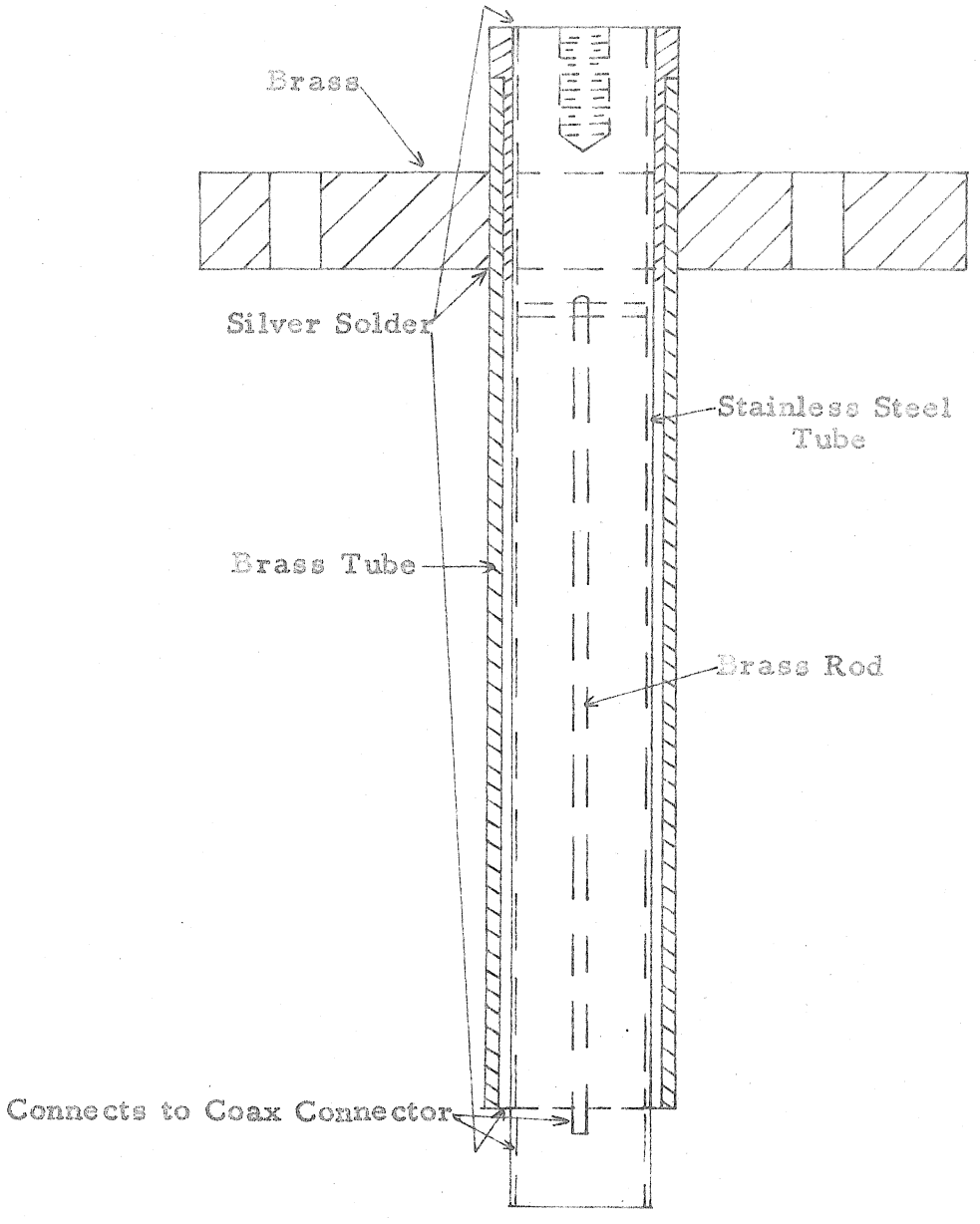

Fig. 3. Non-inductive current-measuring resistor

the divider was quite satisfactory.

The oscilloscope itself was always operated approximately 20 feet away from where the explosion took place. The purpose of the 93 ohm resistor in the circuit was to enable a long coaxial cable to be used from the divider to the oscilloscope input; without it, the cable loaded the divider. The actual voltage division which resulted depended on the length of coax used; with a very short lead it was 108:1 and with 20 feet of RG 62/v it was 165:1. Other voltage dividers were available with division ratios of 10:1 and 1000:1.

A further problem occurred in obtaining the voltage oscillogram. Evidence of what happened is shown in Fig. 34, which shows the voltage and current oscillograms of 3.95 mil diameter iron. During the first microsecond or so, the voltage across the wire rose to about 20,000 volts in this particular case and at later times the voltage across the vaporized wire became of the order of 800 volts. With different wires and different initial conditions, the result was still similar to the above; a very high voltage pulse lasting only a fraction of a microsecond followed by a much smaller voltage signal. Because of interference on the signal which was believed to originate in the thyratron, it was impossible to observe the leading edges of the voltage and current traces. This made little difference in the case of the current trace; because of the circuit inductance, the current had to be a smoothly varying quantity and the oscillogram could be extended back to time zero. In the case of the voltage oscillogram, the voltage could not be measured during this first instant and the initial energy input had to be calculated. The method of calculating this initial energy in-

put is described in Part III.

In obtaining the voltage oscillogram, this high initial positive voltage pulse presented a difficulty because it caused some grid current to flow in the oscilloscope input. This charged the input capacitor of the oscilloscope and the net effect was to bias the grid negatively. In many instances, the grid became so negative that once the pulse was removed, the voltage trace was completely off the screen regardless of its initial setting. This could be offset by using less magnification, but this was unsatisfactory because the resulting magnification often was insufficient for accurate measurements. The difficulty was overcome by using a biased Zener diode at this input to the oscilloscope as shown in Fig. 5. The resistor in this figure was found to make it unnecessary to change the bias to account for the different initial pulses of the different wires.

Oscilloscope

Electrical interference with the measuring equipment presented a serious problem. To prevent ground loops, only one ground was used and the only suitable ground in the laboratory was found to be the hot water radiator. It was necessary to disconnect the high-voltage supply immediately before exploding the wire; if not done, this provided an extra ground and also interference reached the oscilloscope through its power cord. AC line filters were tried for use with the oscilloscope, but the most satisfactory method was to use a two-prong plug instead of the one provided for the oscilloscope, and to use for the one ground of the system a point in the discharge circuit at the place which allowed the oscilloscope to stay at ground potential. Attempts

to enable the oscilloscope to "float" did not succeed. The signal leads to the oscilloscope and the lead to the spark gap were coaxial cables. Metal cabinets of the oscilloscope and of the electronics of the Kerr cell pulser provided additional interference shields.

The oscilloscope used in this research was a Tektronix type 551 double beam Cathode Ray Oscilloscope. This instrument was ideal for the measurements required, as it enabled the current and voltage oscillograms to be taken simultaneously on the same oscilloscope without worry as to phase differences. The rise time of this instrument was faster than needed for this work. The oscilloscope sweep could be adjusted to be free-running or triggered; when triggered it could be made to single sweep and it was used in this mode to obtain the current and voltage oscillograms. All input signals were fed through a delay network in order for the spots to intensify and the sweep to start before the amplified signal was applied to the vertical deflection plates.

To record the traces a Polaroid Land camera was used. The film used in this camera was type 46-L Polaroid film. In order to obtain good records where the spots were moving very fast, a cathode ray tube with a blue phosphorescent material made especially for photographic recording was acquired.

Kerr Cell Camera

This camera was built by A. T. Ellis and is described in detail in Reference 7. The Kerr cell shutter was capable of exposure times of as little as .05 microsecond and repetition rates up to 2×10^6 frames per second. A rotating mirror was used to scan the film with

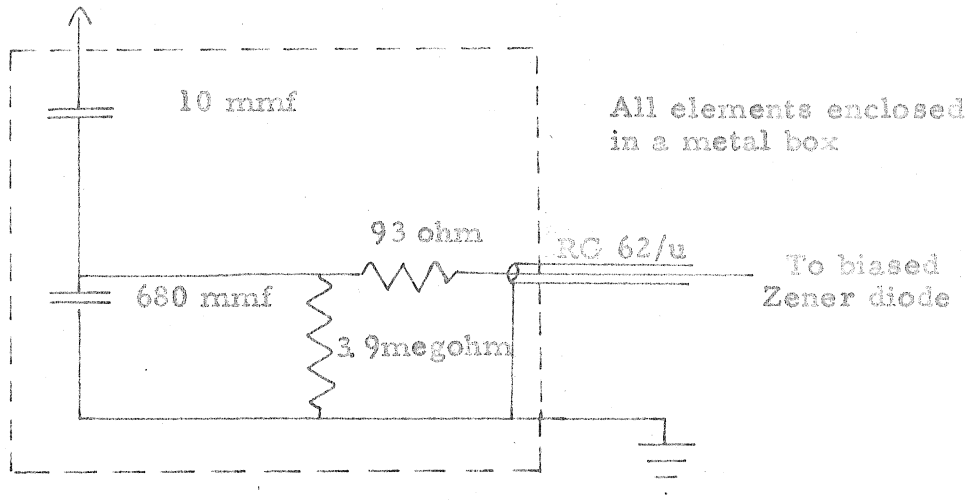

Fig. 4. Voltage divider

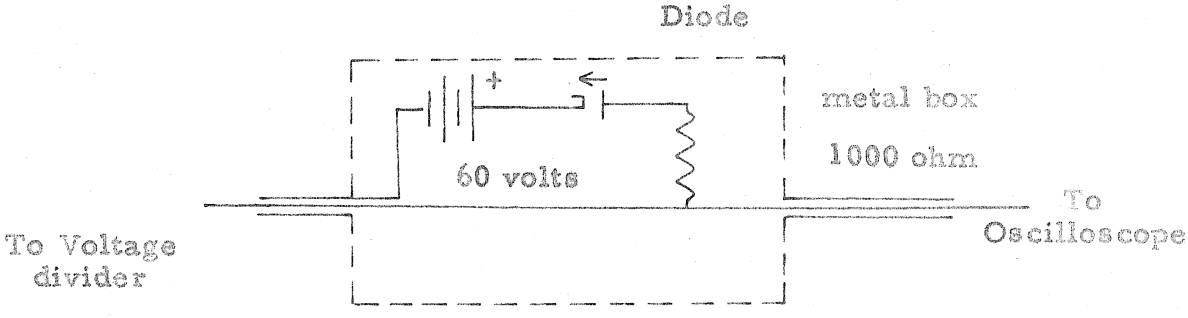

Fig. 5. Biased Zener diode placed at input to oscilloscope

scanning speeds up to 10,000 feet per second. Several choices of lenses were available, the one chosen depending upon the magnification desired. In this experiment the exposure time was .05 microsecond and the speed of rotation of the mirror about 1300 revolutions per second which gave a film scanning speed of about 8000 feet per second. DuPont 928B film was used. It was found that the exploding wire always gave off sufficiently intense light so that obtaining the correct exposures was never a problem.

Light Source

A Beckman No. 8333 hydrogen lamp was chosen to calibrate and standardize the photographic plates containing the exploding wire spectrum. This lamp was specially made for use in the Beckman spectrophotometer which had many requirements in common with those of this application. The regulated power supply used with this lamp was a laboratory constructed model built by K. H. Olsen. This supply gave a DC arc current of 0.3 ampere at 60 - 90 volts. The current through the lamp was constant for input voltage in the range 95 to 120 volts.

Microphotometer

The tracings from an electronic recording microphotometer were used to compare the continuous radiation of the exploding wire with that of the hydrogen lamp whose spectral distribution was determined. This instrument, located in Robinson Laboratory of the California Institute of Technology, used a Leeds and Northrup recorder to trace the density of the continuum. The lowest magnification available was used and this supplied a trace of about 108 cm covering the region

from 2250 Å to 5500 Å. Focusing, alignment, and slit width presented no problems for this application.

Spectrophotometer

A Beckman Model DU spectrophotometer was used to determine the relative spectral energy density of the standardizing lamp. The light was positioned so that the slit of the spectrophotometer was illuminated exactly as when the light was used with the spectrograph. The direct reading mode was used. This spectrophotometer employed a quartz prism, six aluminized surfaces for reflection, and a 1P28 phototube as a detector, all of which had known spectral characteristics.

III. OBSERVATIONS OF EXPLOSIONS IN AIR

The Purpose of the Study

A complete analysis of exploding wire phenomena would be extremely difficult because so many factors are involved. There are complicated end effects, thermoconductivity, viscosity, radiation effects, magnetic and electric effects, and others all acting at once, and it is not easy to isolate a single physical phenomenon for study experimentally in order to aid the analysis. While in principle one could set up simultaneous mathematical relations describing all possible physical processes which could take place in an exploding wire, the result would be so vastly complex that it could not be treated analytically.

Recently, however, a theoretical analysis of the hydrodynamic flow occurring during wire explosions has been undertaken by Carl A. Rouse of the Lawrence Radiation Laboratory[6]. In his original model he assumed instantaneous energy deposition uniformly into a wire at $t = 0$. The purpose of this study was to provide a foundation for further studies when more refinements would be added to the model.

A natural next step in this study was the hydrodynamic flow with a time dependent energy input into the wire and metal vapor. It was partly for this purpose that the observations here of shock wave position, contact surface position, and energy input to the exploding wire as a function of time, were undertaken. Kerr cell pictures of the exploding wire were much better than streak pictures for this purpose because the radius of the contact surface and shock wave may not have been constant along the length of the wire, and they showed immediately the length of wires necessary so that end effects would be negligible

with the particular experimental conditions involved. The first factor was clearly important because of the risk in the streak camera technique of falling on a strong stripe or a situation may have arisen as shown in Fig. 29. When different sizes and types of wires are to be compared as in this study, such variations could easily overshadow differences due to the type of wire. The latter factor was also important and this was a source of concern in Rouse's original study carried out from streak photograph data.

Experimental Technique

There were several methods of rendering the shock wave from an exploding wire visible. Werner Müller, for example, has used Kerr-cell schlieren photography[6]. This method used a double Kerr cell camera in conjunction with special lighting to give schlieren photographs. He made the assumption that the experiment was reproducible, performed the experiment up to one hundred times, and then studied the results of single photographs. Figure 29 is proof that this method could lead to difficulties. Because of the amount of apparatus needed to take schlieren photographs with this method, another method described below was tried first, even though with the Kerr cell apparatus available, repetitive pictures could have been taken.

The method adopted was that first used by Bennett[8] at the Aberdeen Proving Grounds in taking streak photographs, and consisted simply of using a plane mirror for back-lighting the explosion. The mirror was placed about 14 cm behind the wire which was to be exploded and very carefully aligned so that the mirror image of the wire lay directly behind the wire as viewed through the Kerr cell camera

lens. Then, as soon as the wire became luminous, it was effectively illuminated from behind by a light source of the same size. Some of the light from this image which passed through the shock front was refracted by the shock front through a small angle and into the camera lens rendering the shock front visible. The mirror did not have to be exactly 14 cm behind the wire, but this position was chosen after taking a series of pictures using different distances.

Figures 6 through 16 show the results concerning the hydrodynamic flow and power input obtained by exploding different types of wires in air at atmospheric pressure with mirror back-lighting. The wires used are those shown in Table 1 which also lists some of their characteristics. The instrumentation is shown in Fig. 1.

The photographs in Figs. 18 through 29, which illustrate the behavior of the different wires, are overexposed if detail over the contact surface itself were desired, but, because of the back-lighting, this would have been somewhat obstructed anyway. These pictures were taken to obtain data such as presented in Figs. 6 through 16 where it was necessary to follow the shock front position for as long as possible. In these pictures, the length of the wire exploded was 2.4 cm and they were taken with frames $2\frac{1}{2}$ microseconds apart. All of the shock wave data was taken with stored energy of about 3000 joules in a circuit with a ringing frequency of 50 kc.

Better pictures of the wire explosion itself are shown in Figs. 30 and 31 where there was no attempt to photograph the shock wave. Figure 31 is unique; out of more than a hundred such pictures taken, it was the only one which showed the hot wire which had not yet expanded.

Already asymmetries could be noted along the length which gave rise later to the striations that always occurred. Figure 30 shows these striations well. Also, it should be noted that the exploded wire appeared as a hollow cylinder, indicating that the bulk of the gas was close to the contact surface.

Shown in Fig. 17 is a comparison of .003 inch diameter iron wire explosions for initial voltages on the capacitors of 5 kv, 10 kv, and 20 kv. In this case a bank of condensers with a total capacity of 24 microfarads was used in a circuit with a ringing frequency of f = 17.9 kc. These pictures were taken in order to observe the effect of increasing the stored energy upon the wire explosion but without mirror backlighting. It was interesting that, although the power into the wire changed greatly with increased stored energy, the motion of the contact surface was changed only slightly.

Some of the problems associated with obtaining the energy input to the wire as a function of time have already been discussed in the apparatus section. Part of the stored energy was lost electromagnetically, some by resistive heating of the circuit, some by the hydrodynamic flow and radiation produced in the spark gap, some in each unsoldered connection, and the dielectric loss of the capacitors probably accounted for a sizable amount. Only a small fraction of the energy available was absorbed in the wire material. The only method to obtain the instantaneous energy into the wire was by the use of current and voltage oscillograms. These were difficult to obtain reliably because of the high electric and magnetic fields involved.

The current oscillogram is usually obtained with a cathode ray

oscilloscope by measuring the voltage drop across a calibrated resistance placed in series with the wire and this method was used here. Another method sometimes used consists of placing a small coil near the wire and integrating the signal obtained. By use of the former method an independent check on the result was available be cause the total charge which flowed during the first half cycle should have been nearly twice that stored in the capacitor bank. With the resistor used in this experiment, it was necessary to correct for its inductance.

The voltage oscillogram was obtained by connecting the voltage divider across the wire and current resistor. The current resistor was included because of the point chosen to be ground. The small contribution of the current resistor to the voltage signal was then subtracted. The rate of change of current in the exploding wire circuit often exceeded 10^{10} amperes/second, and in any attempt to measure the voltage across an exploding wire care had to be taken to eliminate, or compensate for, the induced emf developed across the measuring circuit. However, the induced emf due to the self-inductance of the wire was included in the voltage measurement, and likewise the overvoltage due to the change in the inductance of the wire as it ruptured and expanded, since the latter represented energy being transferred back into circuit from the magnetic field as it collapsed. In order to make certain that the induced emf developed across the measuring circuit made a negligible contribution to the oscillograms, a wire was exploded with the lead from the voltage divider to the exploding wire disconnected at the discharge circuit, but with the remainder of the circuit undisturbed. In that case no signal appeared on the cathode ray tube,

and it was concluded that the voltage measured was indeed the voltage across the wire. As mentioned before, high frequency noise blanked the oscilloscope traces for about a microsecond. An attempt was made to filter this noise, but with no success.

The power input into the wire at the instant of vaporization could be roughly calculated using data given in Table 1. Experiments using pulsed currents have shown that Ohm's law held at current densities up to approximately 10^8 amperes/cm^2, which was a little higher than that attained here at the time that the wire gasified. The power input was calculated as follows:

$$W = \int_o^{t_o} R_{av} I^2 \, dt = R_{av} I_o^2 \frac{t_o^3}{3} \; ; \; t_o = \sqrt[3]{\frac{3W}{R_{av} I_o^2}}$$

where

W was the total energy required to vaporize the wire from Table 1;

R_{av} was the average resistance during the solid and liquid phase - very nearly equal to the resistance at the end of the liquid phase, R_f, since most of the energy was added at this point because of large heats of vaporization;

$I = I_o t$ was the current which could be considered to rise linearly for times less than 1 microsecond; and

t_o was the time of wire vaporization or explosion.

From the above, the power input, P_{t_o}, at t_o was

$$P_{t_o} = I^2 R_f = R_f \left(\frac{3 W I_o}{R_{av}} \right)^{2/3}$$

where R_f was the resistivity at the end of the liquid phase. While the contribution of the self-inductance of the wire to the voltage developed across it could easily have been added to this calculation, its contribution was quite small and so was neglected. However, in view of the short duration of this process, it was reasonable to expect that deviations from ordinary melting and evaporation might have occurred. In the above calculation, it was not important that the solid may have superheated; even if the liquid did superheat considerably the result would not have been affected greatly, since the largest contribution to W in every case was the latent heat of vaporization. It has been suggested that the temperature does rise far above the normal boiling point before the change to a gaseous state occurs[10]. For copper, silver, and aluminum, the data concerning shock front and contact surface position obtained from different explosions of the same type of wires showed some spread from the mean values which have been plotted. Tungsten and iron, on the other hand, were quite reproducible and had extremely well defined boundaries. If there were considerable superheating this would explain the behavior of the copper, silver and aluminum, because for these, exactly the same amount of superheating would not be expected in each explosion.

The power input curves shown in Figs. 6 through 16 were obtained from voltage and current oscillograms such as those shown in Fig. 36 and extended down to $t_o = 0$ with the aid of the above method. In the case of tungsten, sufficient information about the metal was not available to calculate the power input when the wire gasified.

Figure 34 is the photograph that was obtained by placing a thick piece of plate glass with its edge perpendicular to the wire and a short distance away at the side of the wire. It was thought that perhaps the reflected shock would create a visible disturbance propagating through the explosion products, but none was detected.

Results

The results of these experiments are presented graphically on the following pages.

TABLE 1

Physical Properties of the Wires and Calculation of Initial Energy Input

Type of wire and diam. (mils)	Density g/cm^3	Mass of wire (2.4 cm length) milligrams	Melting point °C	Boiling point °C	Heat of fusion cal/g	Heat of Vaporization cal/g	Resistance 2.4 cm length ohms (20°C)	Energy needed to vaporize wire joules	R_{av} ohms (est)	R_f ohms	Power into wire at end of evaporation megawatts	Time when evaporation becomes complete microseconds
3.95 Fe	7.87	1.470	1535	2900	65.1	1580	.308	13	3.0	3	114	.41
3.0 Fe	7.87	.860	1535	2900	65.1	1580	1.18	7.7	5.5	6.3	93	.29
2.0 Fe	7.87	.383	1535	2900	65.1	1580	.53	3.4	12	14.3	71	.17
2.0 Ag	10.5	.51	960	2180	25.3	557	.19	1.5	2.0	2.4	23	.24
1.0 Ag	10.5	.127	960	2180	25.3	557	.76	.4	8.0	9.6	15.3	.10
3.15 Cu	8.92	1.07	1084	2500	48.9	1250	.075	6.9	1.2	1.45	55	.46
2.0 Cu	8.92	.433	1084	2500	48.9	1250	.18	2.7	3.0	3.6	40	.25
1.0 Cu	8.92	.108	1084	2500	48.9	1250	.74	.4	12.0	14.4	25.5	.10
2.0 W	19.32	.94	3382	6000	61	-	.63	-	-	-	-	-
0.50 W	19.32	.059	3382	6000	61	-	10	-	-	-	-	-
1.0 Al	2.70	.033	660	2500	93.5	2580	1.27	.5	40	48	31	.06

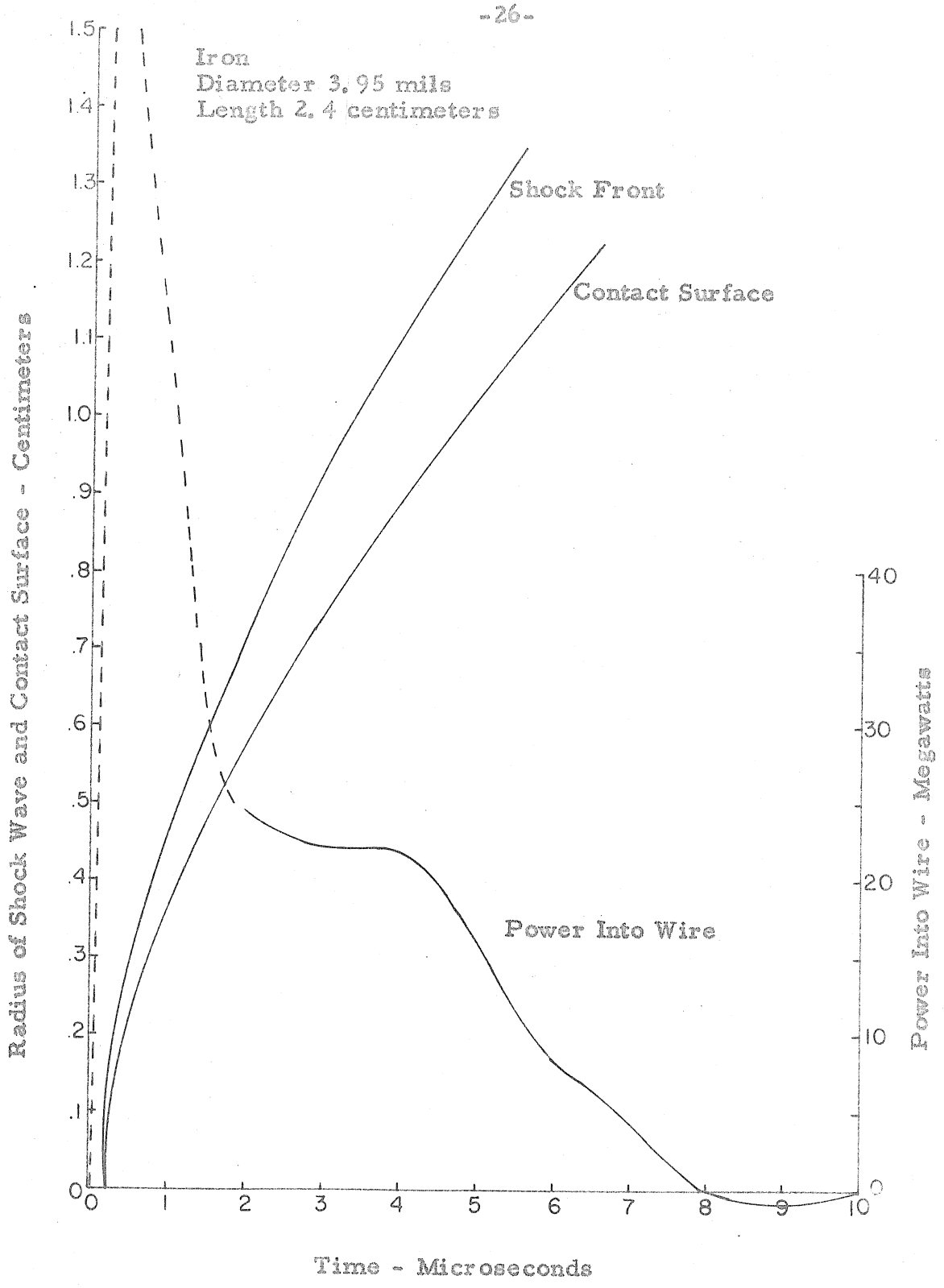

Fig. 6. Hydrodynamic flow data

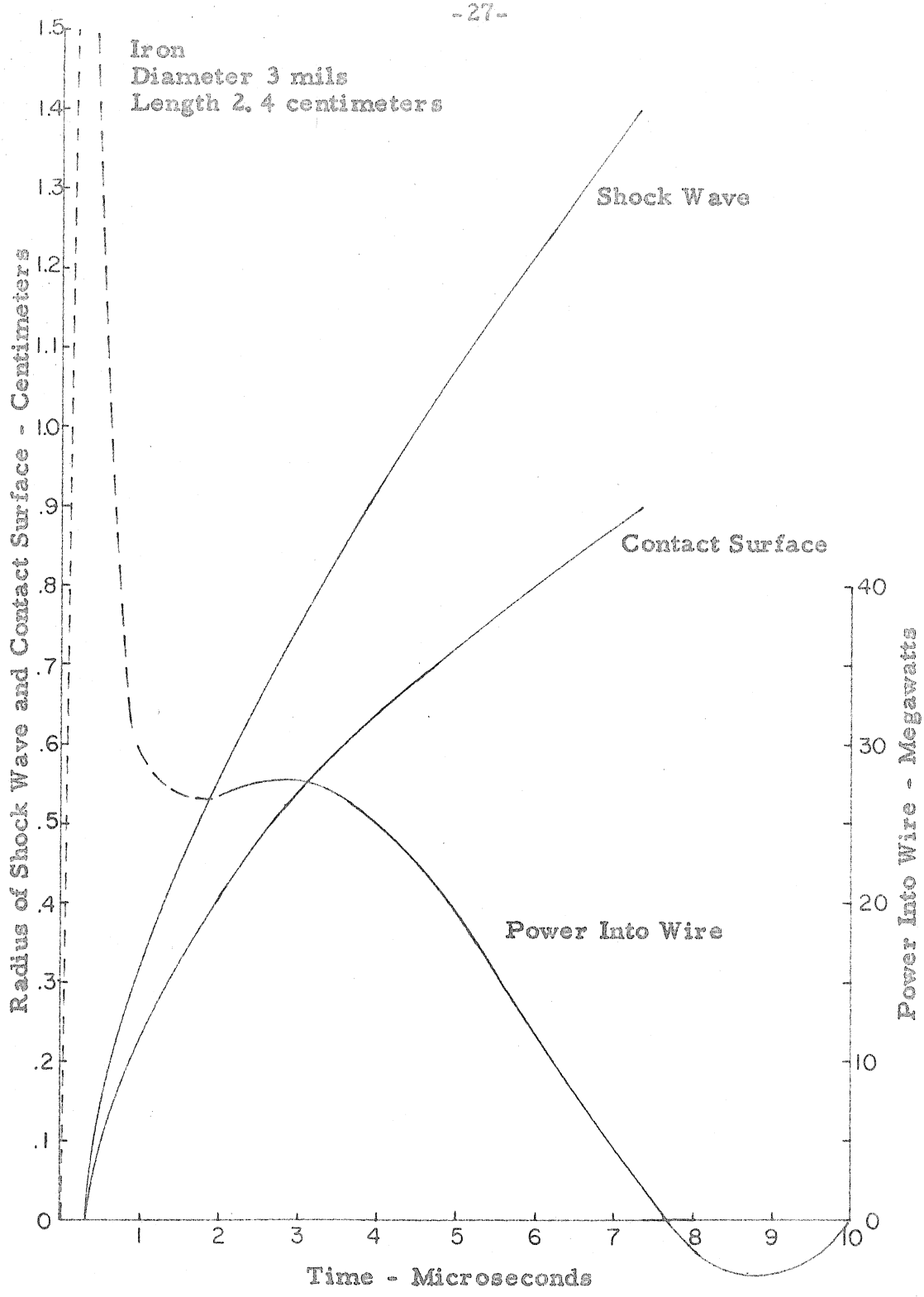

Fig. 7. Hydrodynamic flow data

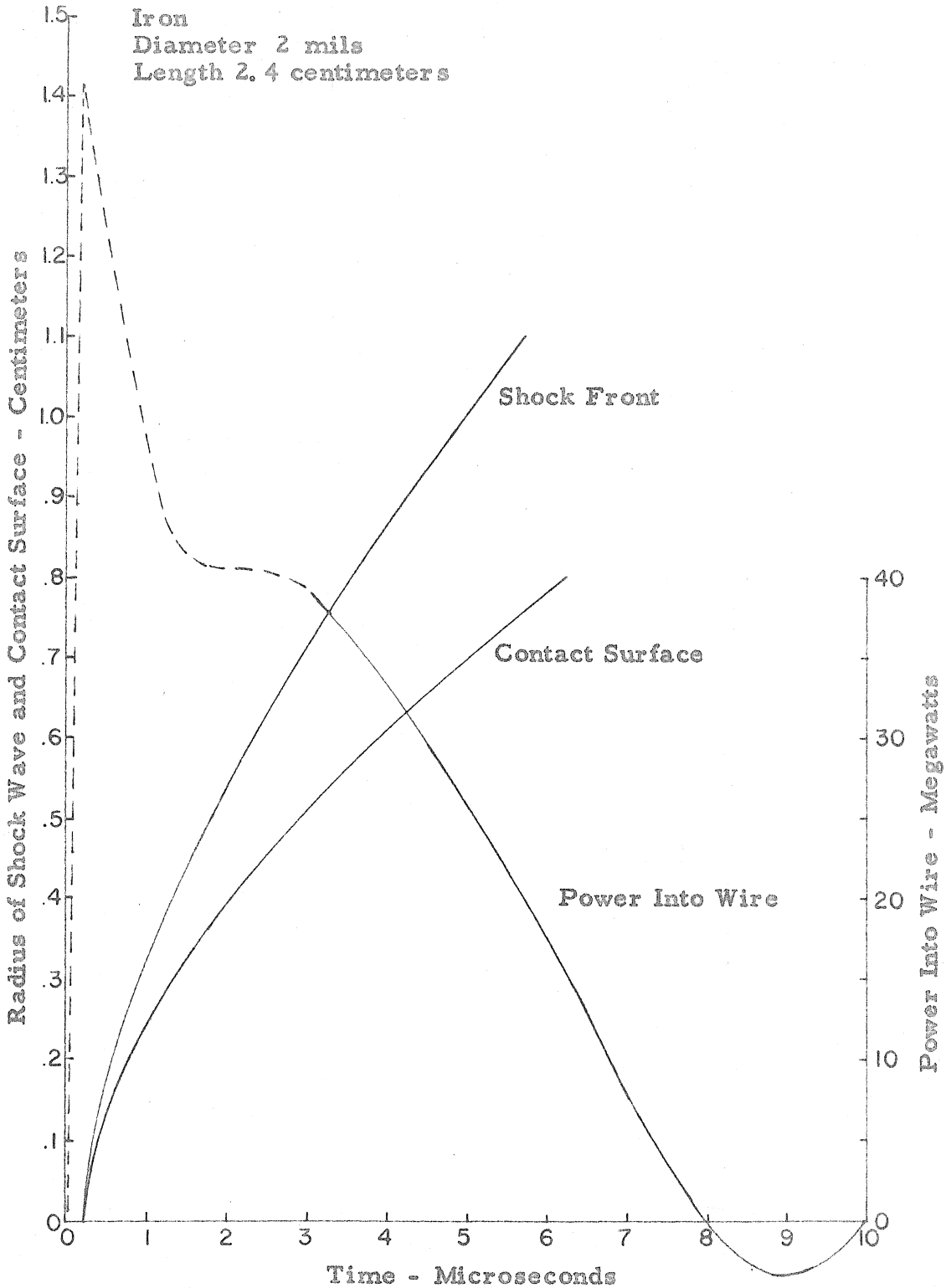

Fig. 8. Hydrodynamic flow data

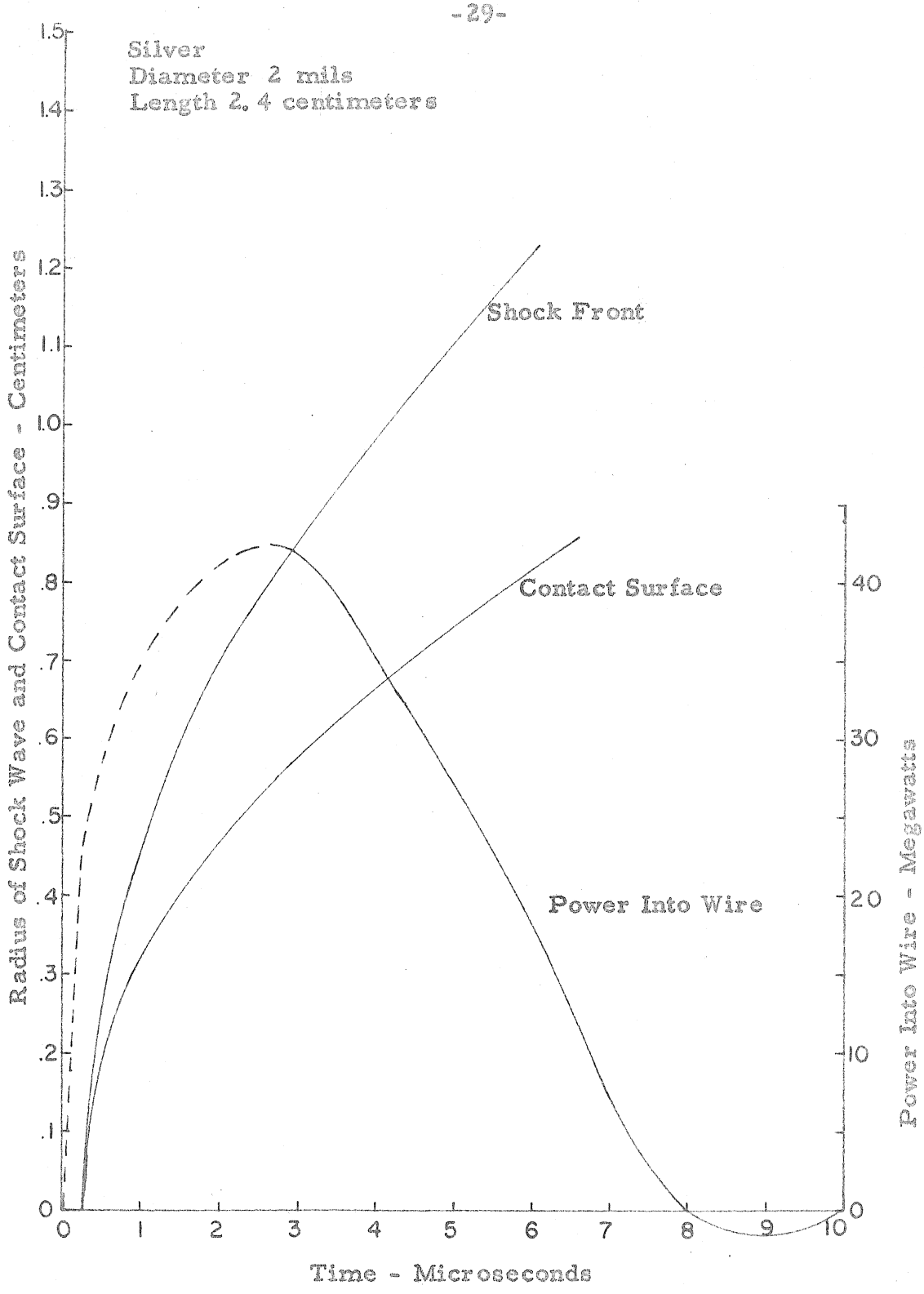

Fig. 9. Hydrodynamic flow data

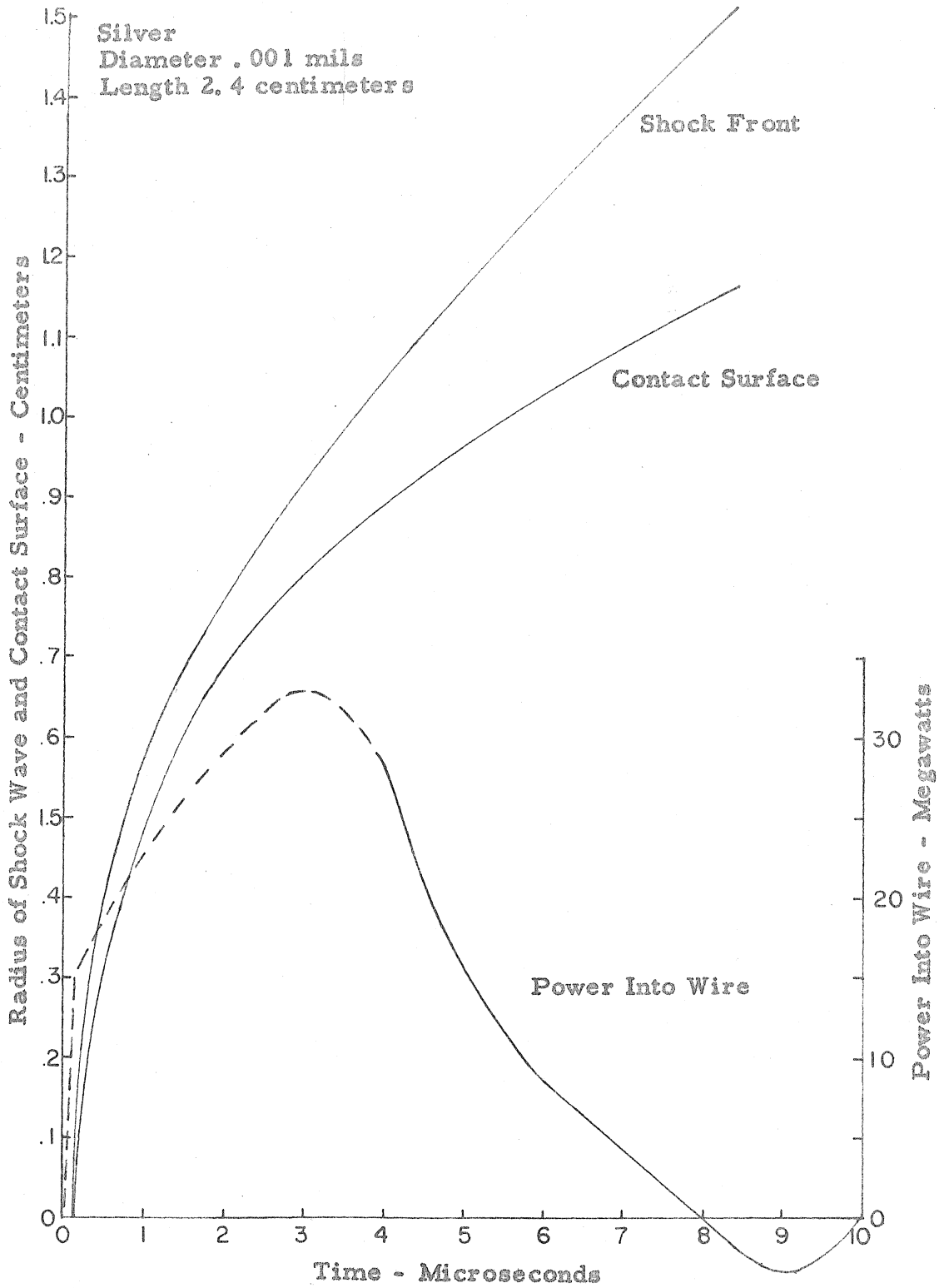

Fig. 10. Hydrodynamic flow data

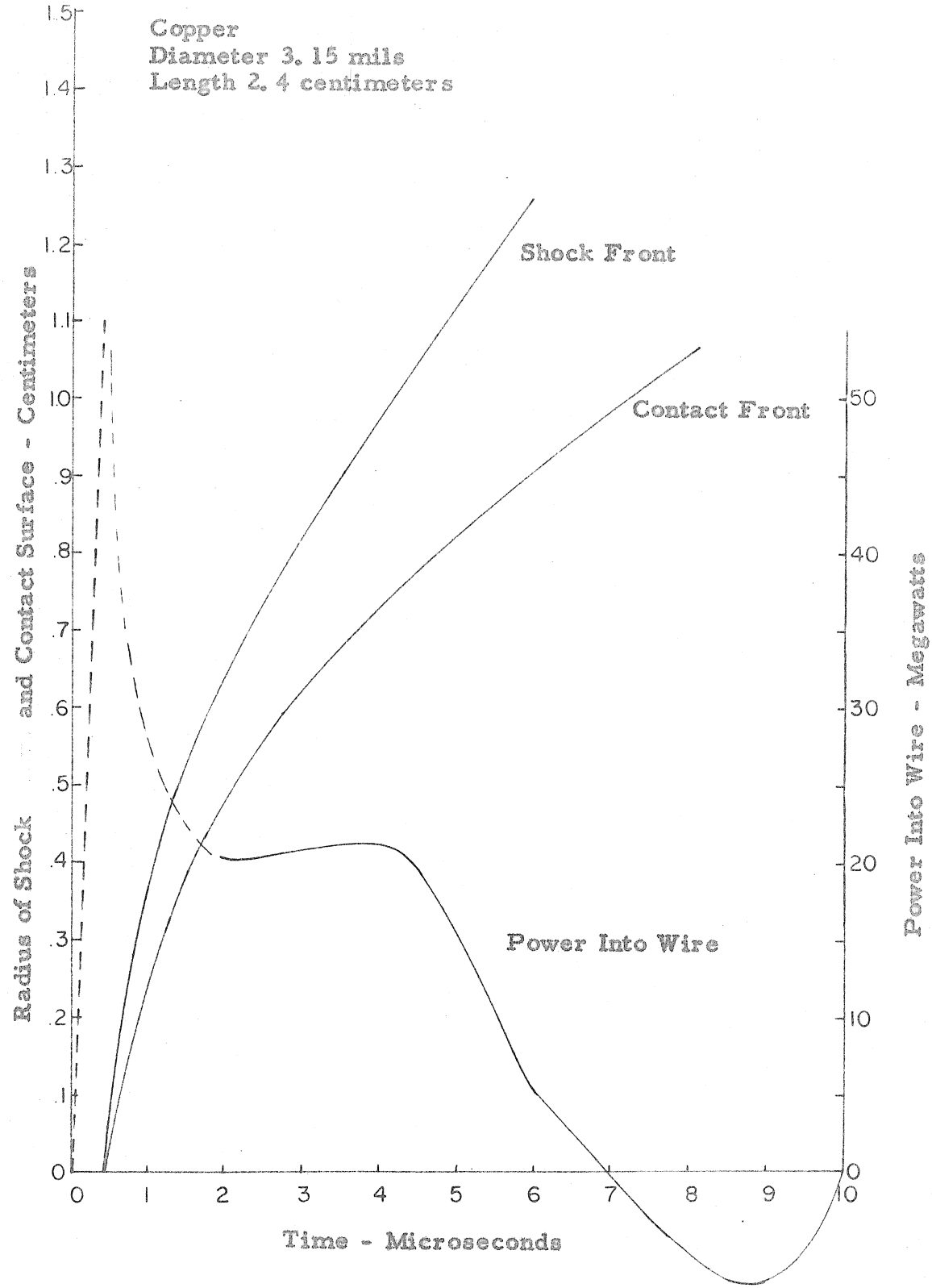

Fig. 11. Hydrodynamic flow data

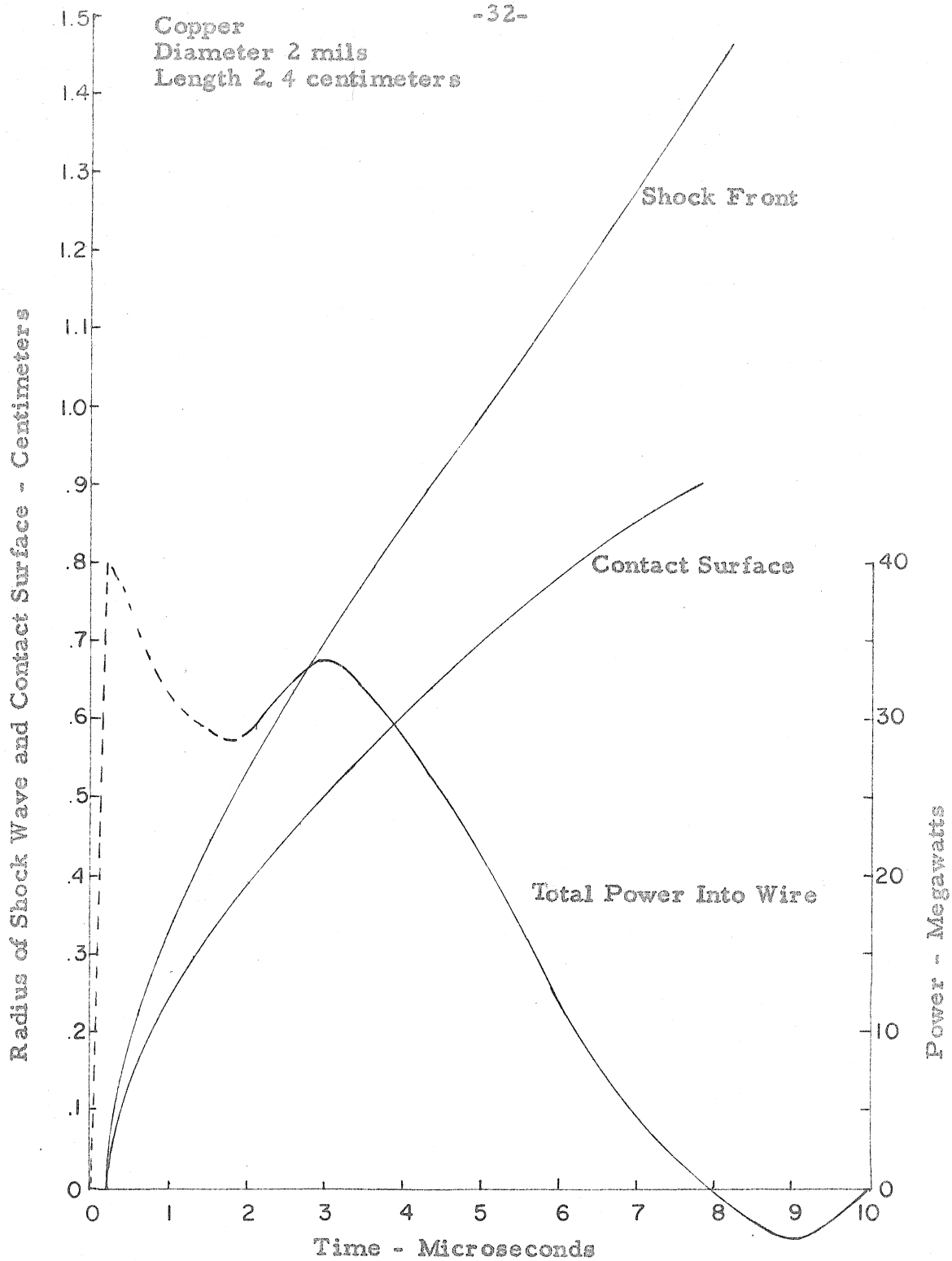

Fig. 12. Hydrodynamic flow data

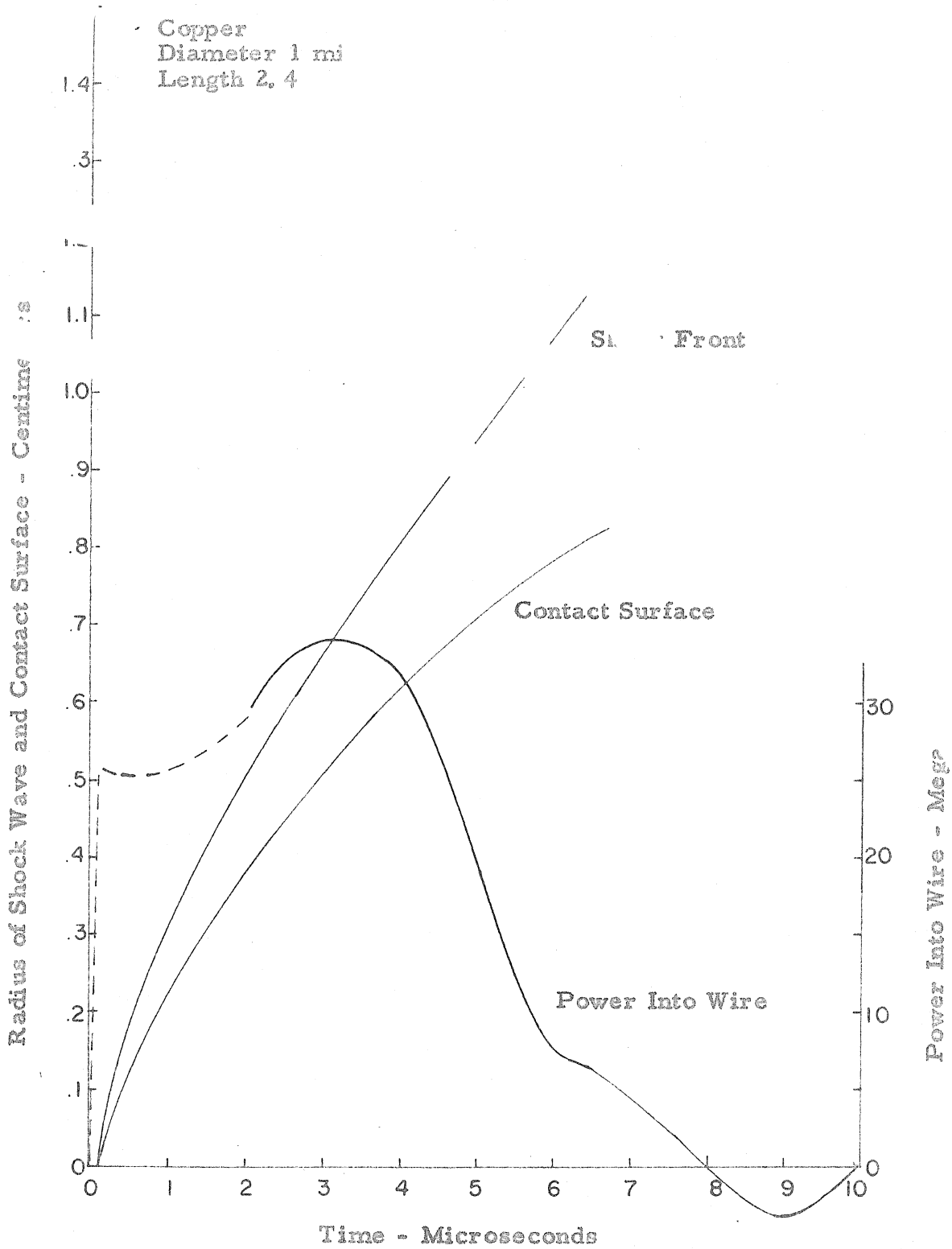

Fig. 13. Hydrodynamic flow data

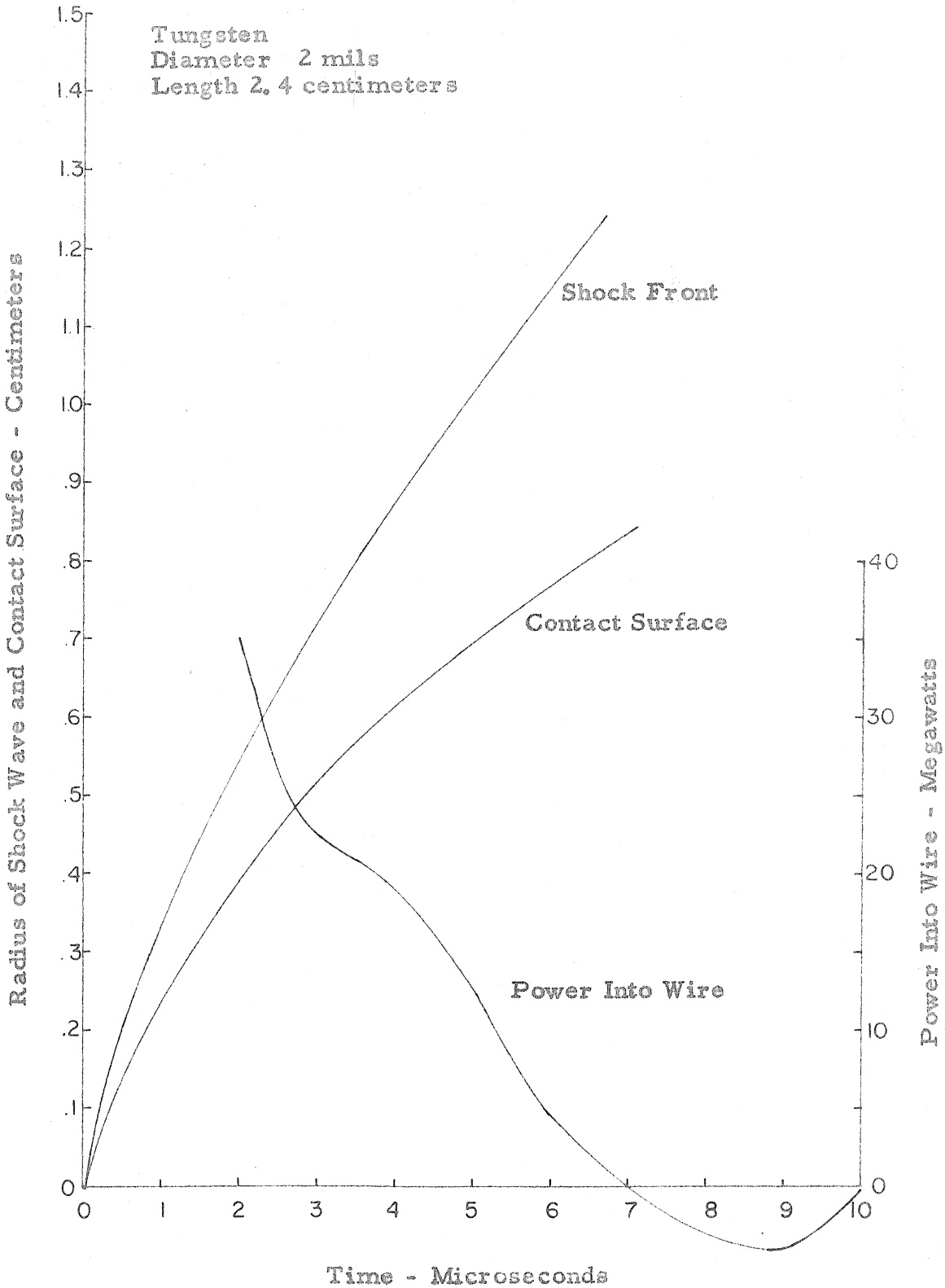

Fig. 14. Hydrodynamic flow data

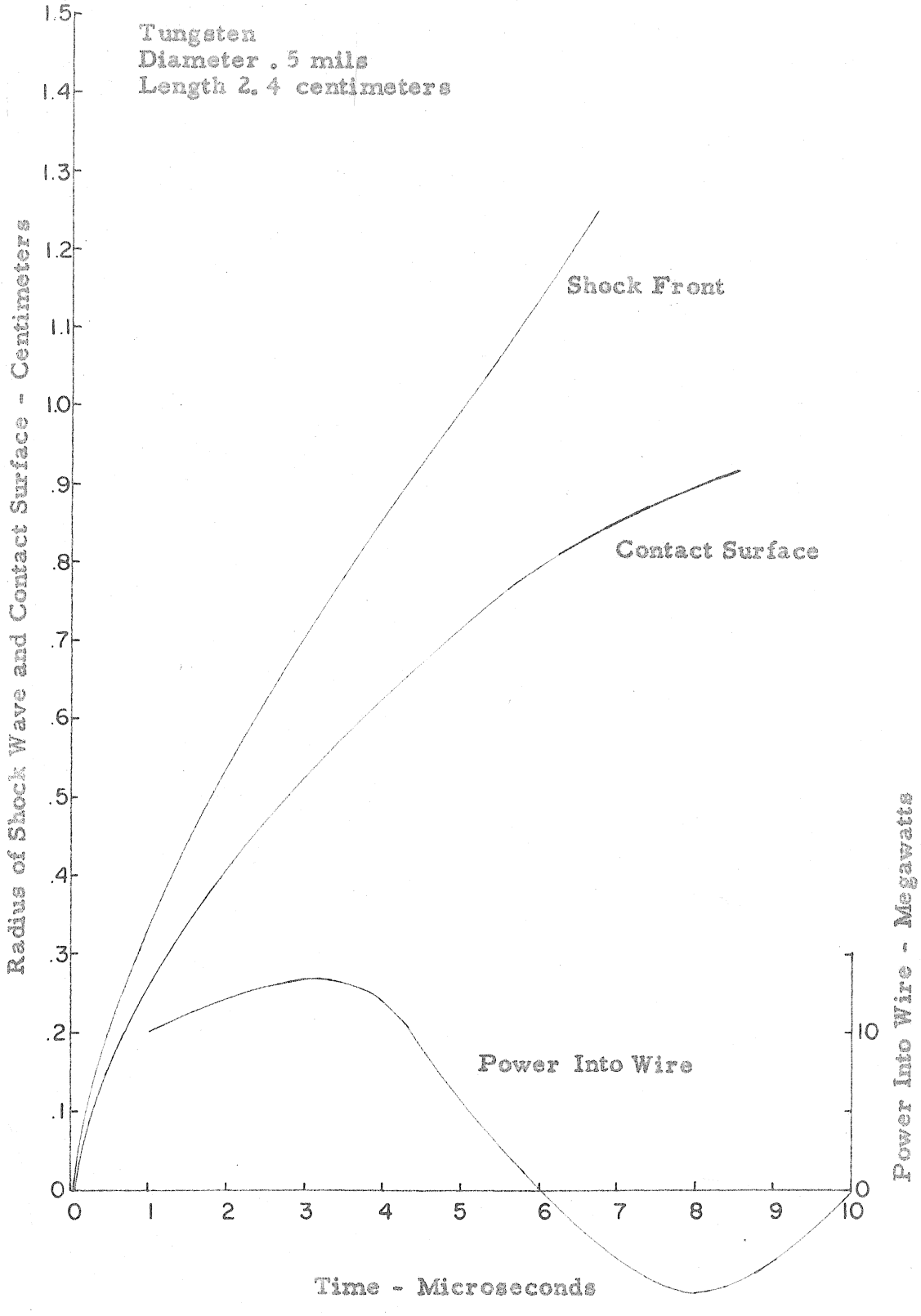

Fig. 15. Hydrodynamic flow data

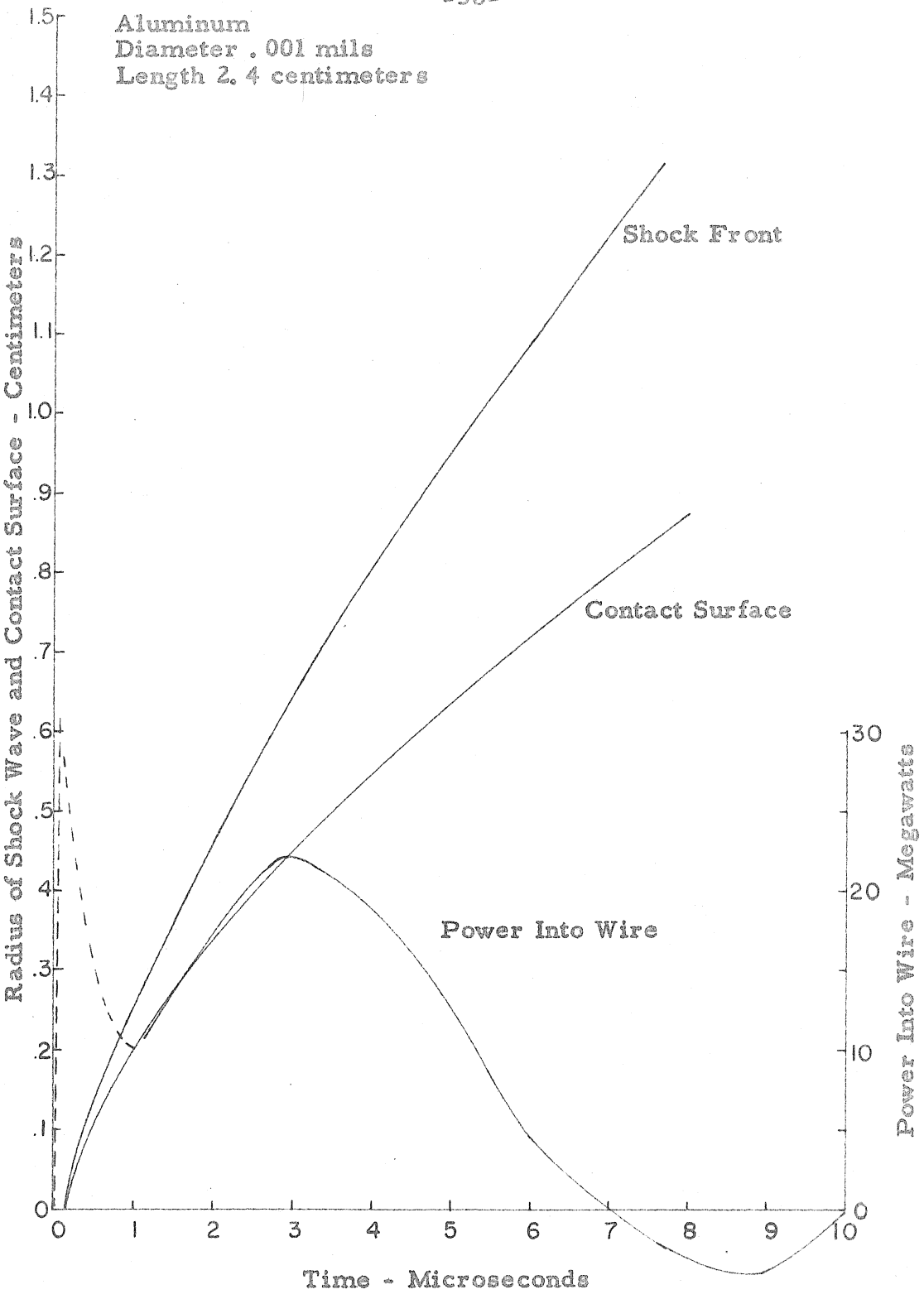

Fig. 16. Hydrodynamic flow data

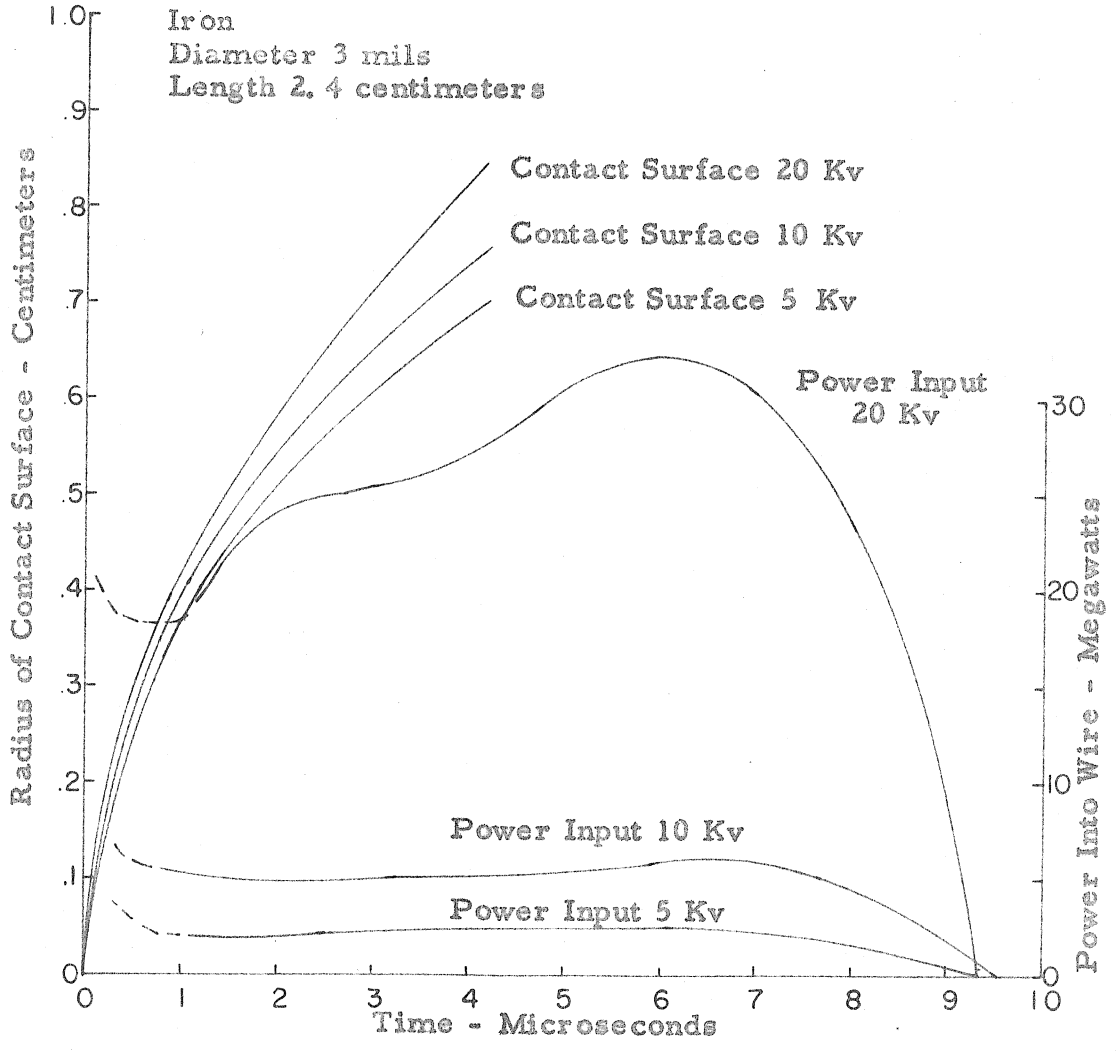

Fig. 17. Comparison of results for different initial voltages on capacitors

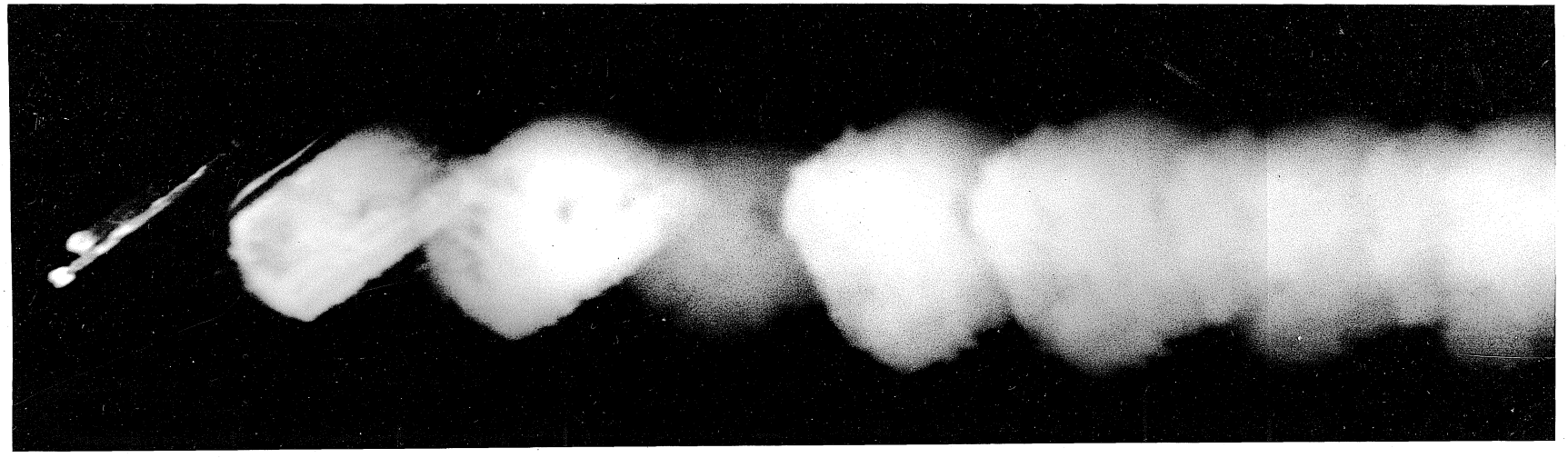

Fig. 18. Kerr cell photograph of 3.95 mil diameter iron wire in air

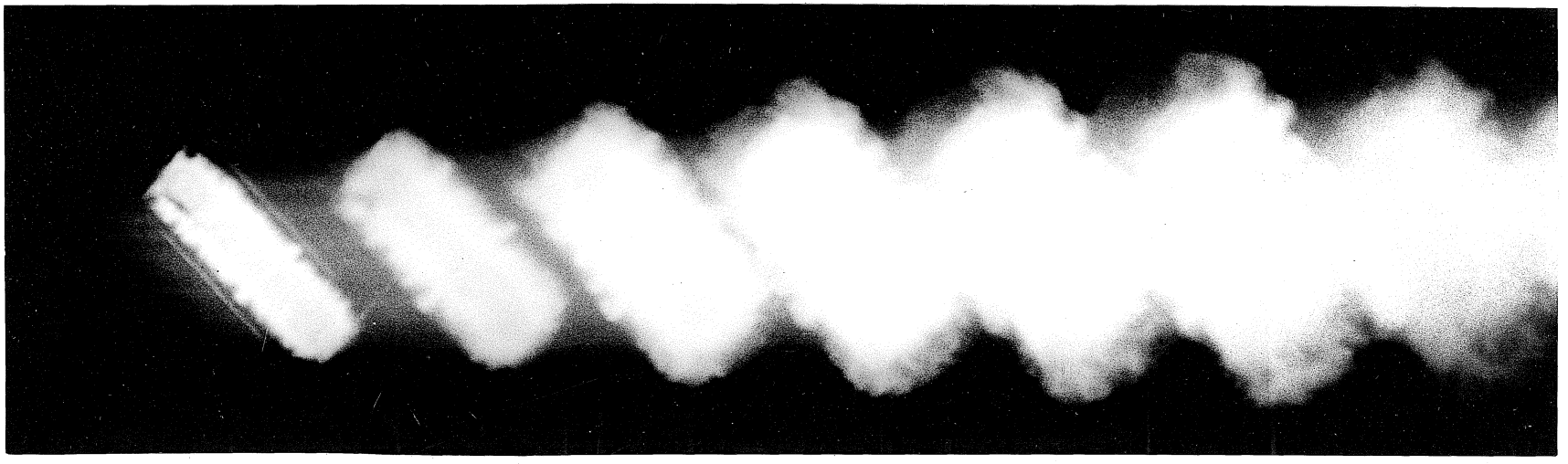

Fig. 19. Kerr cell photograph of 3.0 mil diameter iron wire in air

Fig. 20. Kerr cell photograph of 2.0 mil diameter iron wire in air

Fig. 21. Kerr cell photograph of 2.0 mil diameter silver wire in air

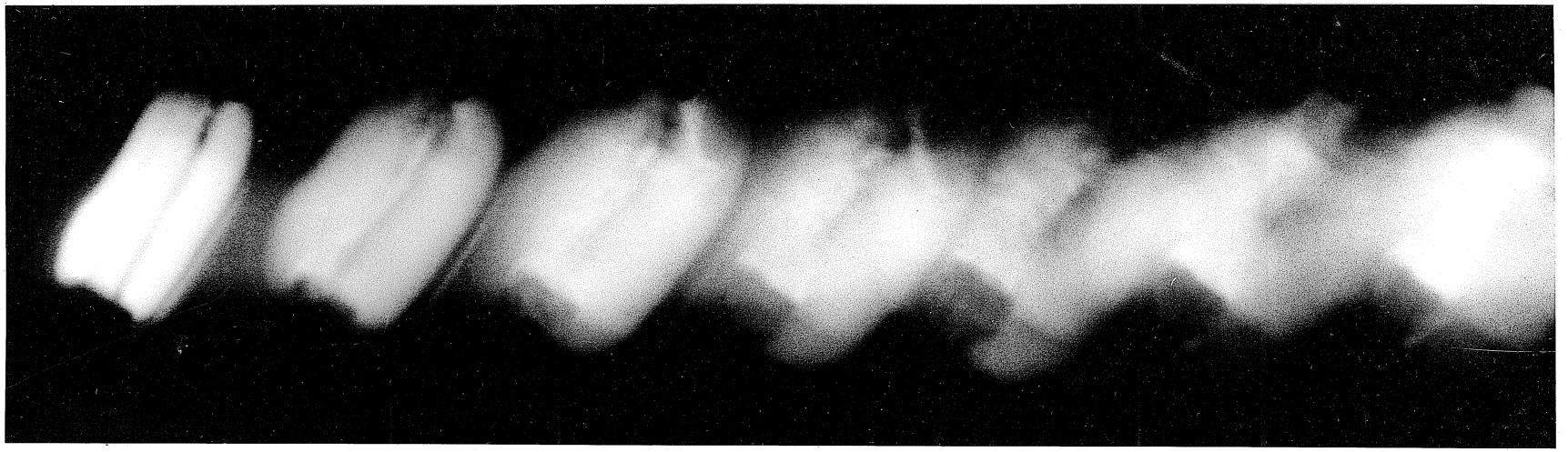

Fig. 22. Kerr cell photograph of 1.0 mil diameter silver wire in air

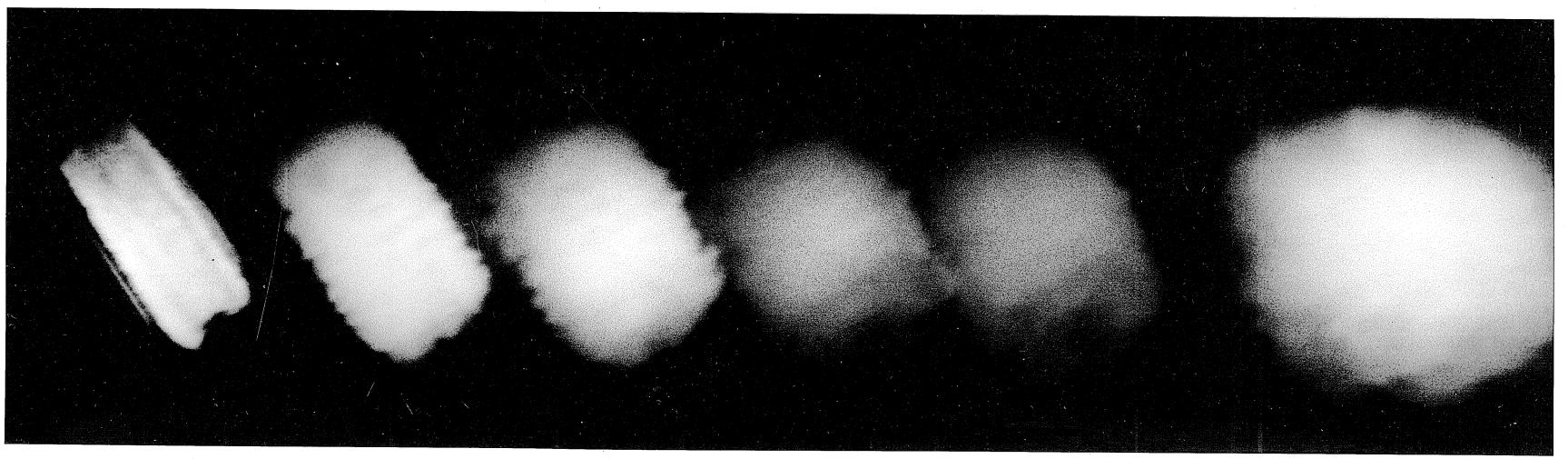

Fig. 23. Kerr cell photograph of 3.15 mil diameter copper wire in air

Fig. 24. Kerr cell photograph of 2.0 mil diameter copper wire in air

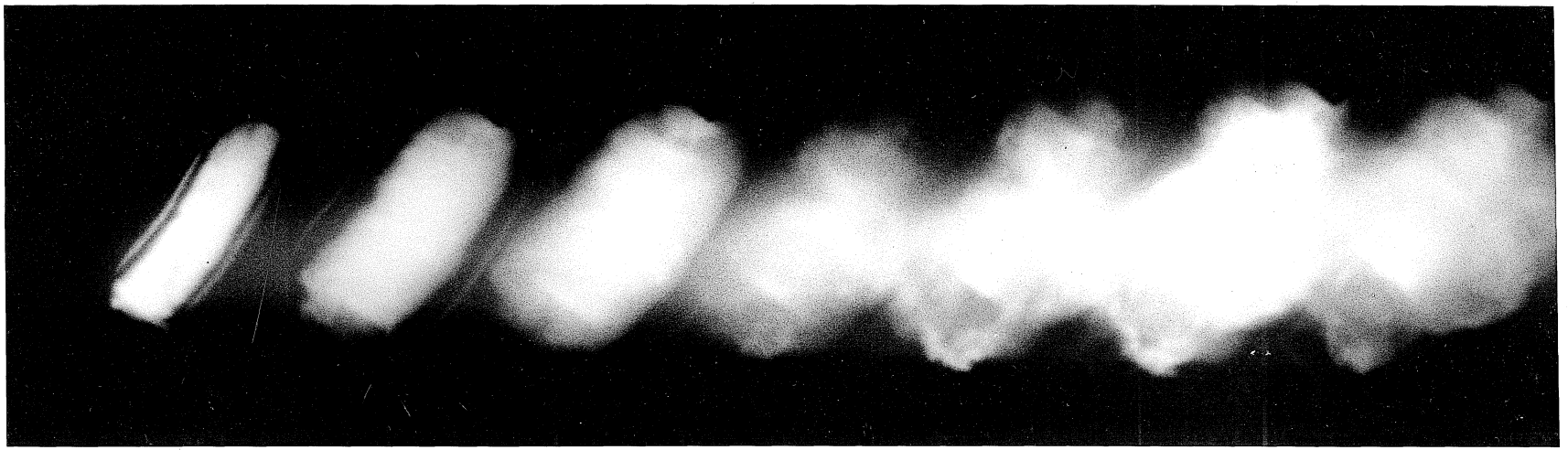

Fig. 25. Kerr cell photograph of 1.0 mil diameter copper wire in air

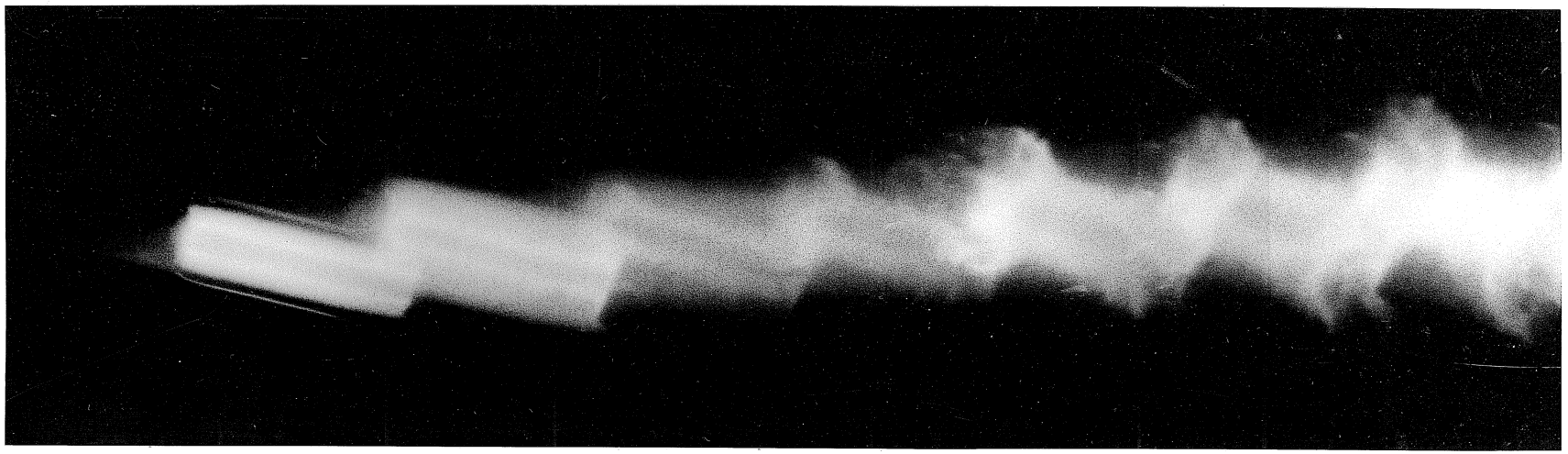

Fig. 26. Kerr cell photograph of 2.0 mil diameter tungsten wire in air

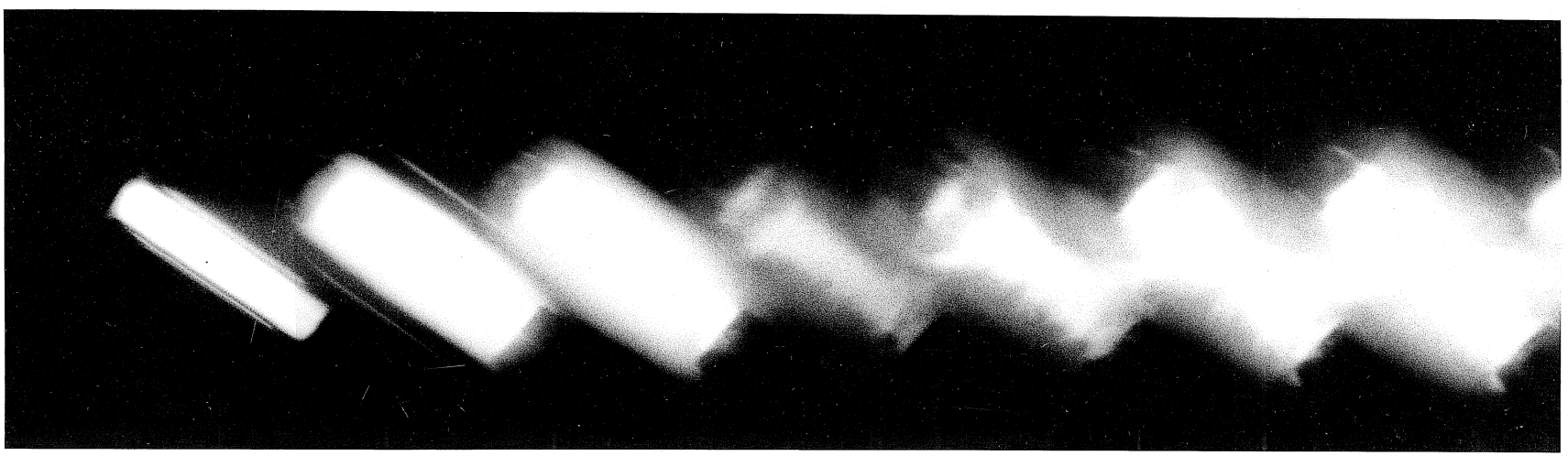

Fig. 27. Kerr cell photograph of 0.5 mil diameter tungsten wire in air

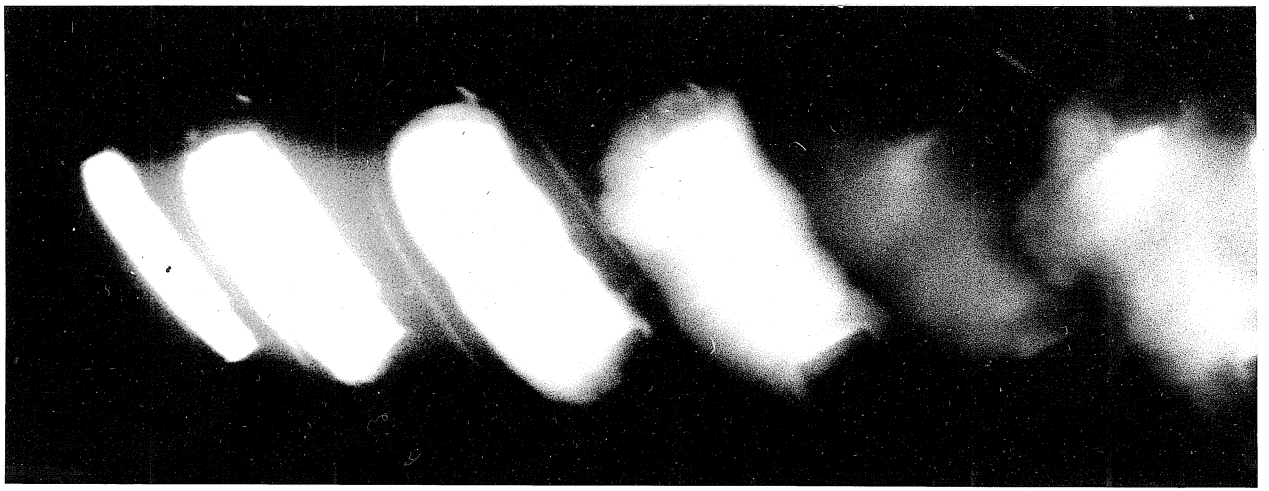

Fig. 28. Kerr cell photograph of 1.0 mil diameter aluminum wire in air

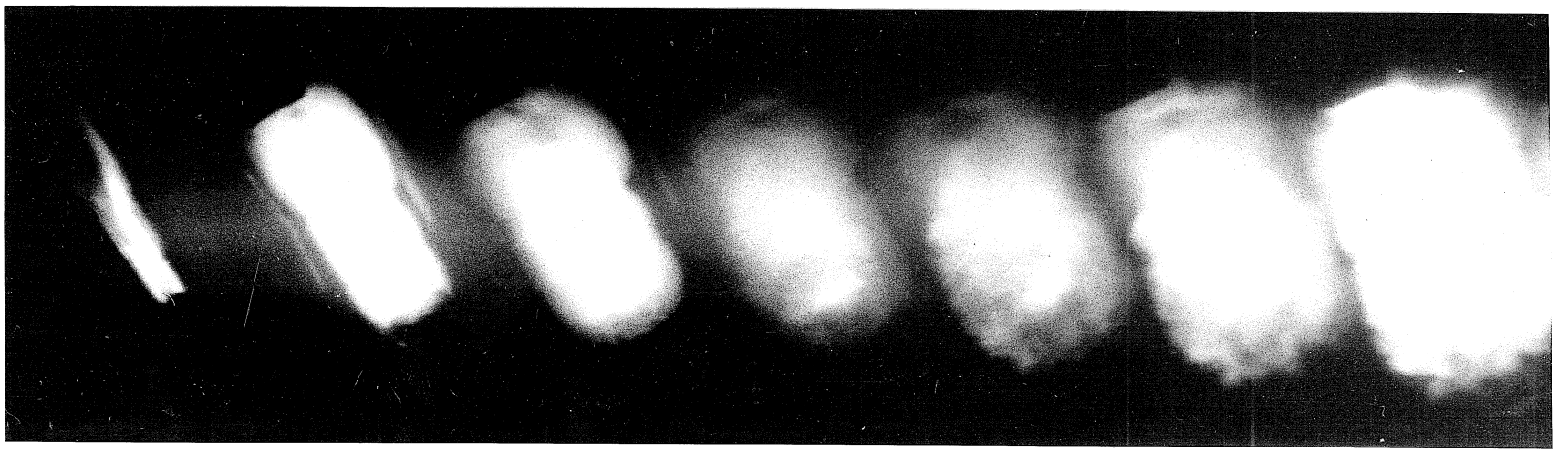

Fig. 29. Asymmetries along length, 1.0 mil diameter silver wire

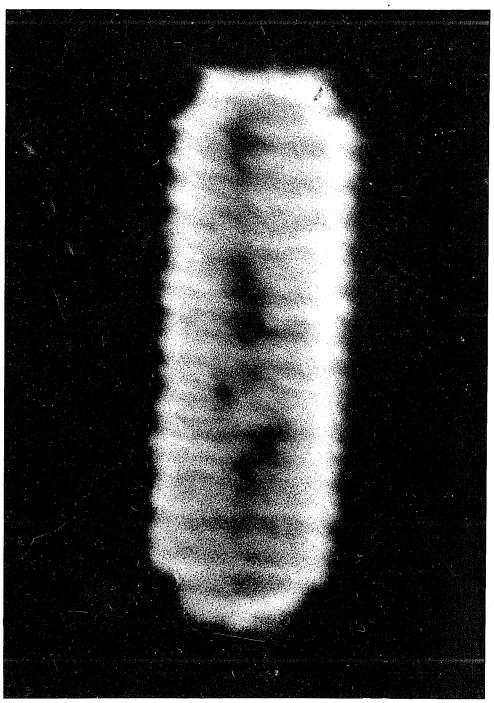

Fig. 30. Example of striations

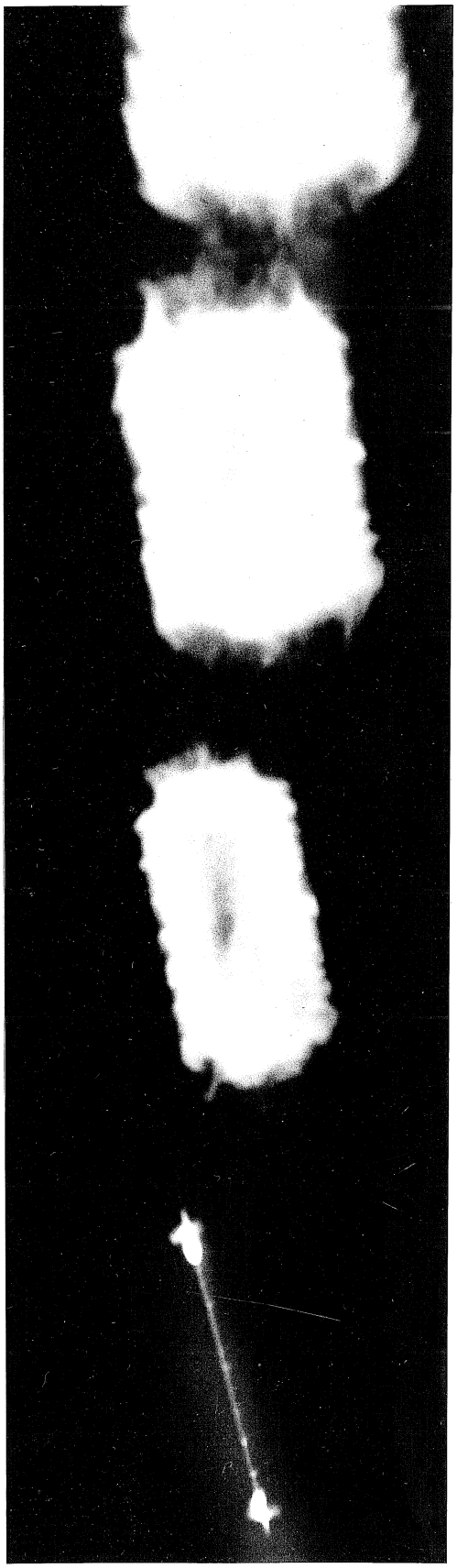

Fig. 31. Wire as it begins to explode

Fig. 32. Obstacle in path of explosion

Fig. 33. Streak Photograph

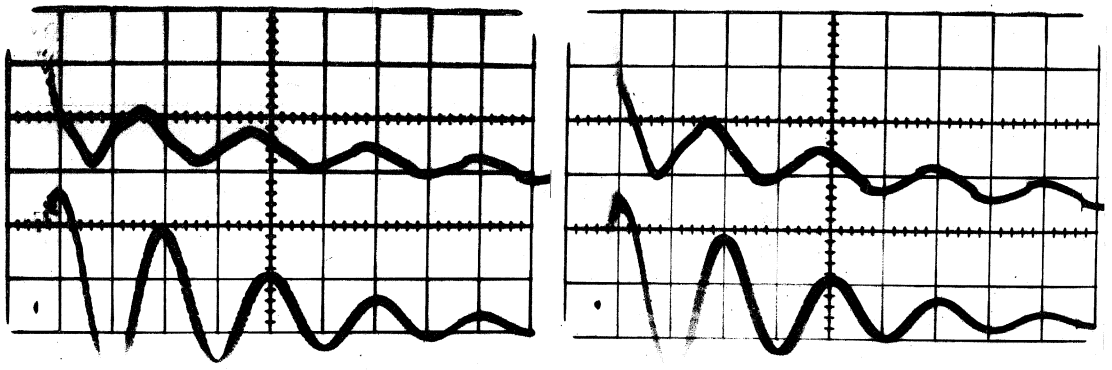

3.95 mil diameter iron

2.0 mil diameter iron

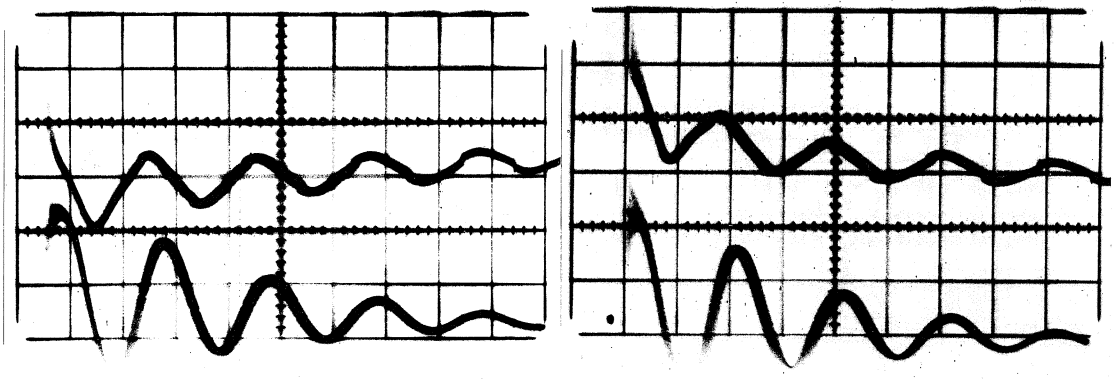

2.0 mil diameter tungsten

2.0 mil diameter silver

Fig. 34. Voltage (top trace) and current (bottom trace) oscillograms

IV. HYDRODYNAMIC FLOW COMPUTING

Purpose

It was shown by Rouse in Reference 6 that it was possible, using a simplified model, to calculate the hydrodynamic flow in exploding wire phenomena. This model was modified so that a time dependent energy input and a calculated variable gamma law equation of state could be considered. If the hydrodynamic flow could be duplicated with such a theoretical model, then such quantities as the pressure, velocity, and density distributions given by the theoretical model should be nearly the same as those in the experiment. Aside from the above consideration, it was illuminating to compare the energy input necessary to produce the hydrodynamic flow in the theoretical case with that measured. These were not expected to be identical because the theoretical energy input represents only that which goes essentially into the hydrodynamic flow, while the measured energy input accounted for all energy losses such as radiation, heating of electrodes, etc.

Method

The method used was very similar to that presented by Rouse[6] for the case of instantaneous energy deposition, and for that reason only the modifications of that analysis are presented here. The system of differential equations solved were changed in that

$$\frac{2E}{\partial t} = \frac{p}{\rho^2} \frac{\partial \rho}{\partial t}$$

was modified to

$$\frac{\partial E}{\partial t} = \frac{p}{\rho^2} \frac{\partial \rho}{\partial t} + S(t)$$

where S(t) was the power input per unit mass which was deposited uniformly throughout the mass of the wire. The boundary conditions and the artificial viscosity term remained unchanged. The initial conditions became:

$$\gamma_o = .003985 \text{ cm}$$

$$E^o_{cu} = .16 \frac{\text{joules}}{\text{cm}^3}$$

$$E^o_{air} = .250 \frac{\text{joules}}{\text{cm}^3}$$

$$\rho^o_{cu} = 8.90 \text{ g/cm}^3$$

$$p^o_{cu} = 1.07 \times 10^6 \frac{\text{dynes}}{\text{cm}^2}$$

$$p^o_{air} = 10^6 \frac{\text{dynes}}{\text{cm}^2}$$

$$\text{Initial volume of wire} = .5 \times 10^{-4} \frac{\text{cm}^3}{\text{cm of wire}}$$

$$\text{Initial mass of wire} = 4.45 \times 10^{-4} \frac{\text{gm}}{\text{cm of wire}}$$

Radius of cylinder of air equal in mass to that of copper = 0.333 cm

The model used can be described as follows. At t = 0 it was assumed that energy began to be deposited in the copper wire, surrounded by air at STP, in accordance with the form of S(t). The equation of state of the copper wire, given in tabular form by Rouse in Reference 11, was obtained from a solution of Saha's equation. No change of state for the copper was assumed. The air was assumed to obey the theoretical equation of state, also in tabular form, calculated

by F. R. Gilmore[12]. End effects, radiation diffusion, thermo-conductivity, real viscosity, mixing of metal vapor and air, magnetic effects, and non-uniform current distribution were neglected.

Results

Two sets of calculations were performed. The hydrodynamic flow results along with the assumed power input for the first calculation are shown in Fig. 35. The first power input was chosen proportional to the square of the current, given by $(2E_o/\tau)\sin^2\pi t/\tau$, and the second because it approximated the measured power input. It should be noted when comparing the theory and experiment that the power input shown here is per centimeter of wire length while those values in Part III are the total power into wires of length 2.4 centimeters. Comparison of Fig. 36 and Fig. 11 shows that not only was the total energy into the wire too large in calculation I, but it went in too slowly at first.

The second set of calculations used a power input as shown in Fig. 37 which also gives the resulting hydrodynamic flow. In this case the agreement with experiment was much better and very encouraging. While the agreement was not perfect, it was near enough so that the pressure, density, and velocity from the calculations were expected to approximate those of the experimental setup. These quantities are plotted in Figs. 37, 38 and 39.

An interesting result was apparent from a comparison of the results in Reference 6 with those presented in Figs. 35, 36 and 11. With

instantaneous energy deposition the calculations show the contact surface lagged behind those of the experimental case, while when the energy was deposited too slowly, the contact surface was farther advanced than in the experimental case.

Unfortunately, it did not appear possible to get an estimate of some of the other energies involved such as radiation, end effects, etc. for two reasons. First, the energy input measurement was uncertain at the very early times, and second, as can be seen from a comparison of the results of calculations I and II, as shown in Figs. 35 and 36, changes in the hydrodynamic flow became relatively insensitive to changes in the energy input at these large energy values.

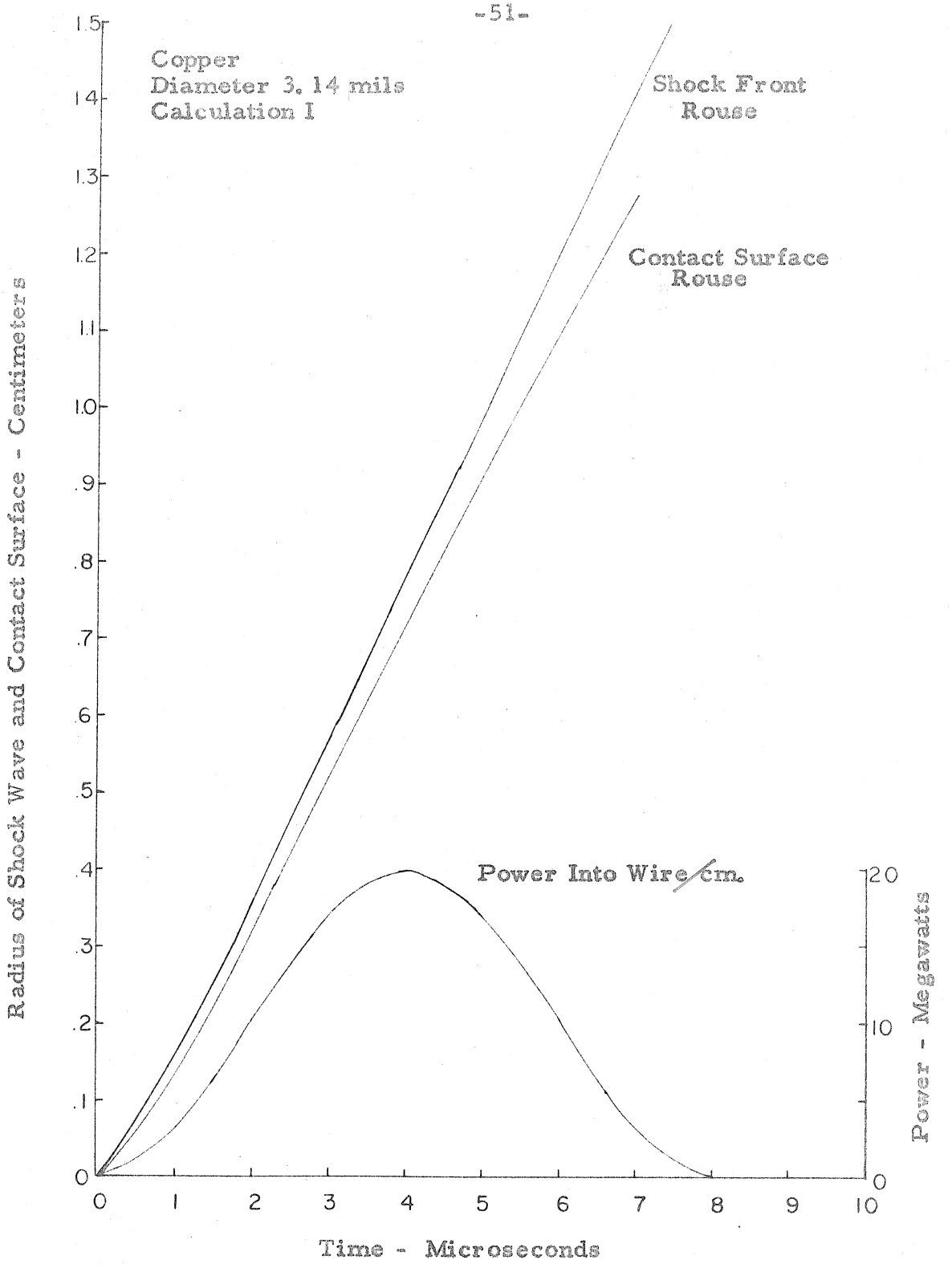

Fig. 35. Calculated hydrodynamic flow

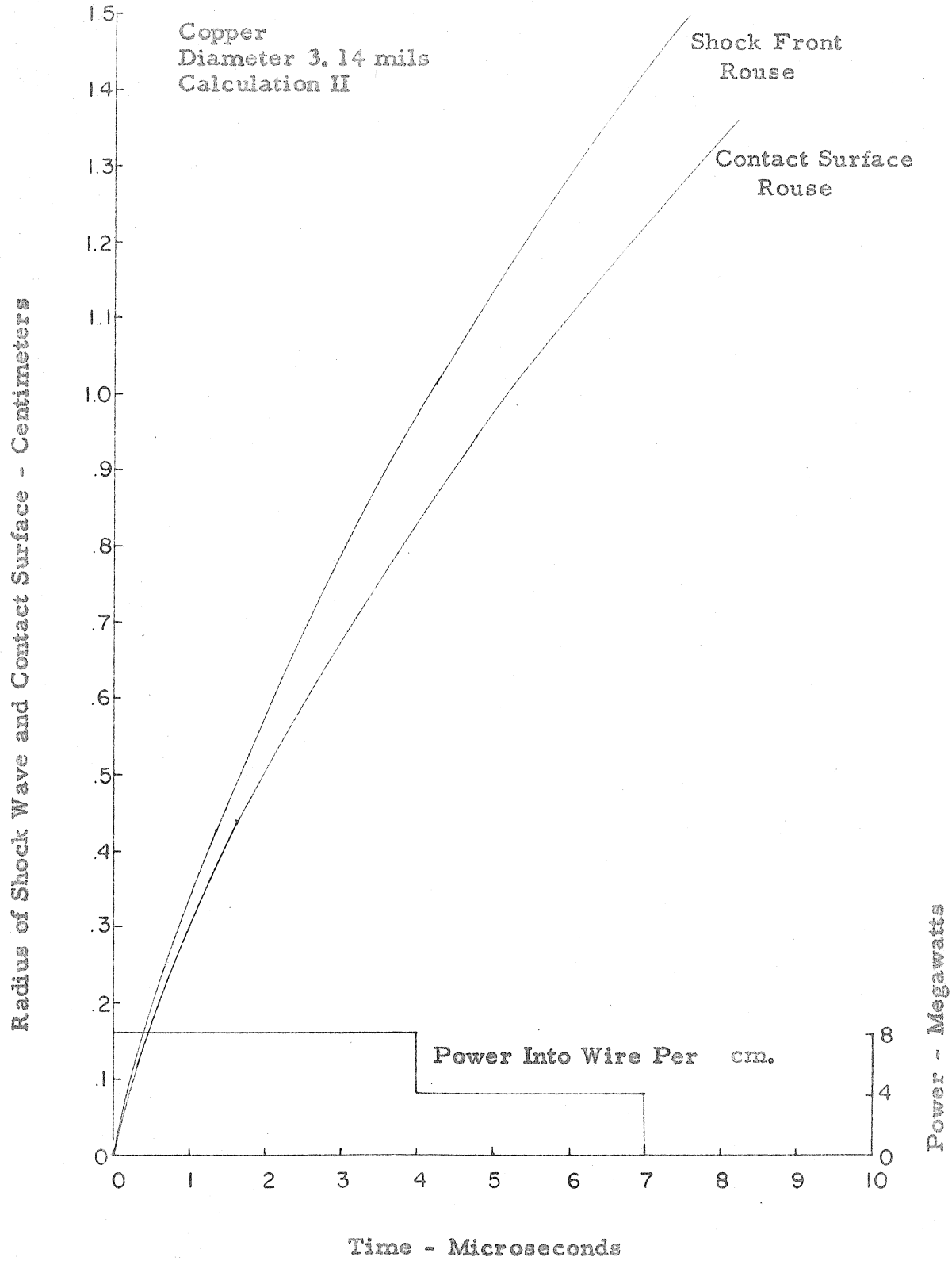

Fig. 36. Calculated hydrodynamic flow

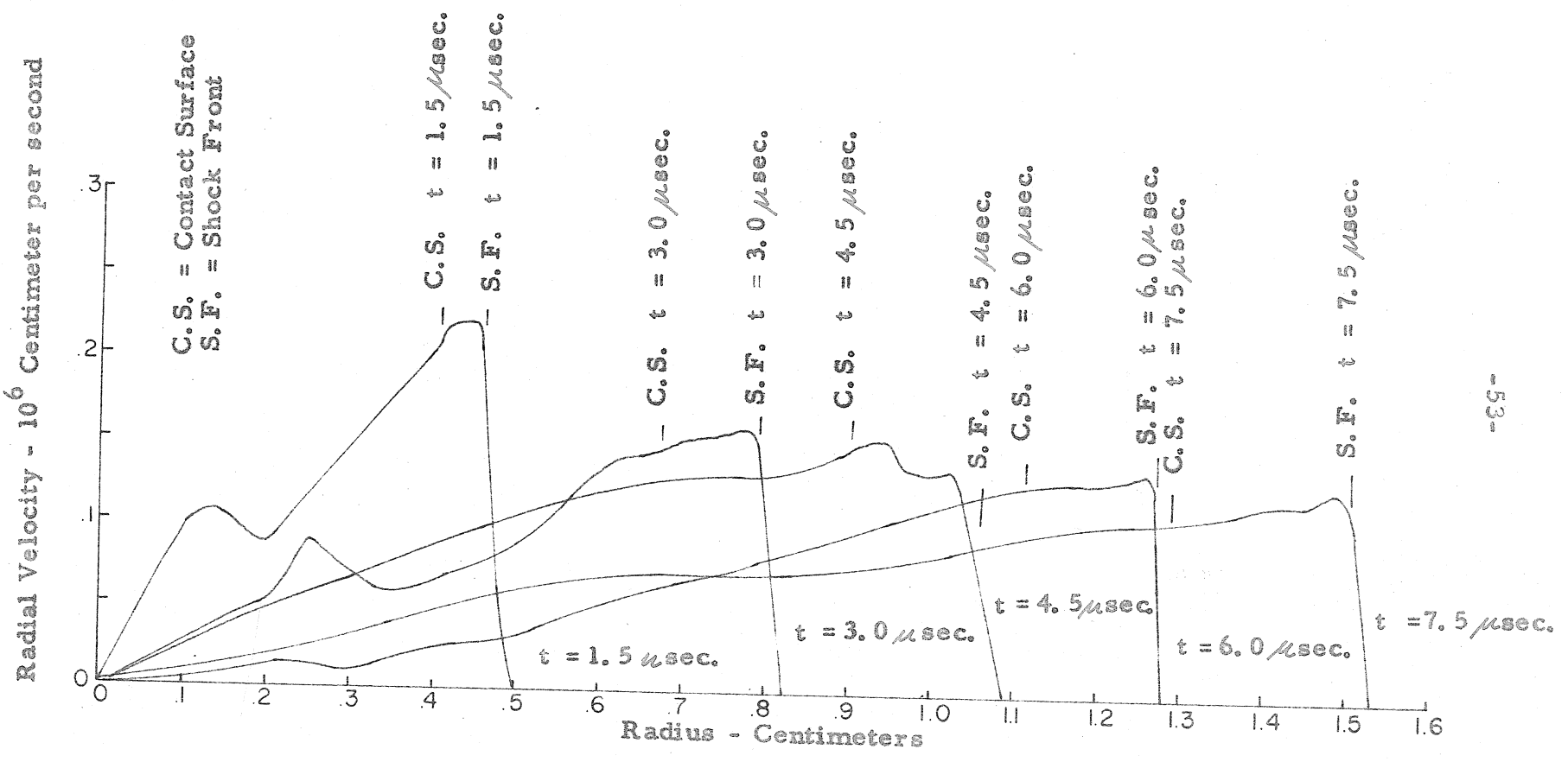

Fig. 37. Radial velocity profile at different times from Calculation II

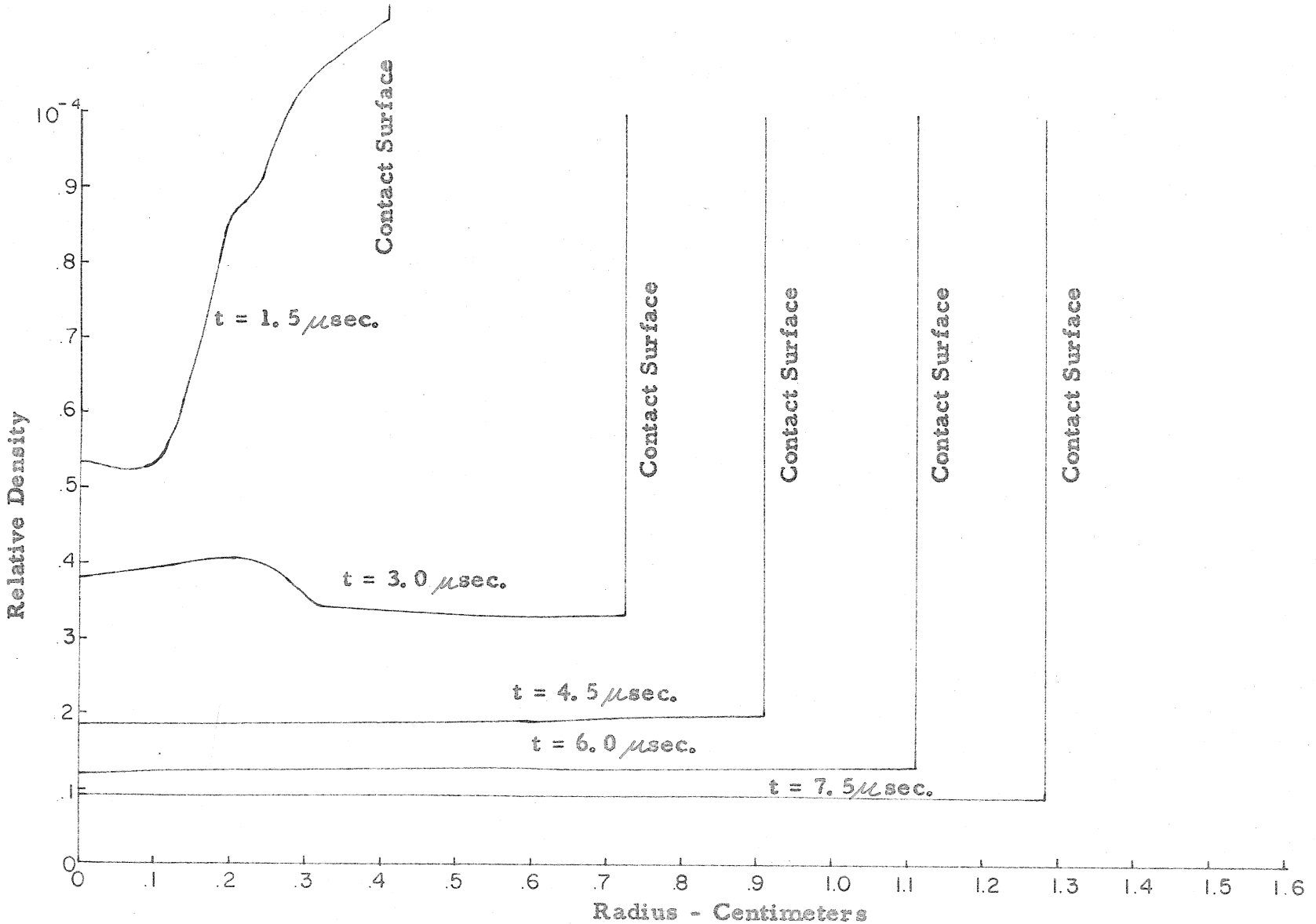

Fig. 38. Relative density profiles in the copper for different times from Calculation II

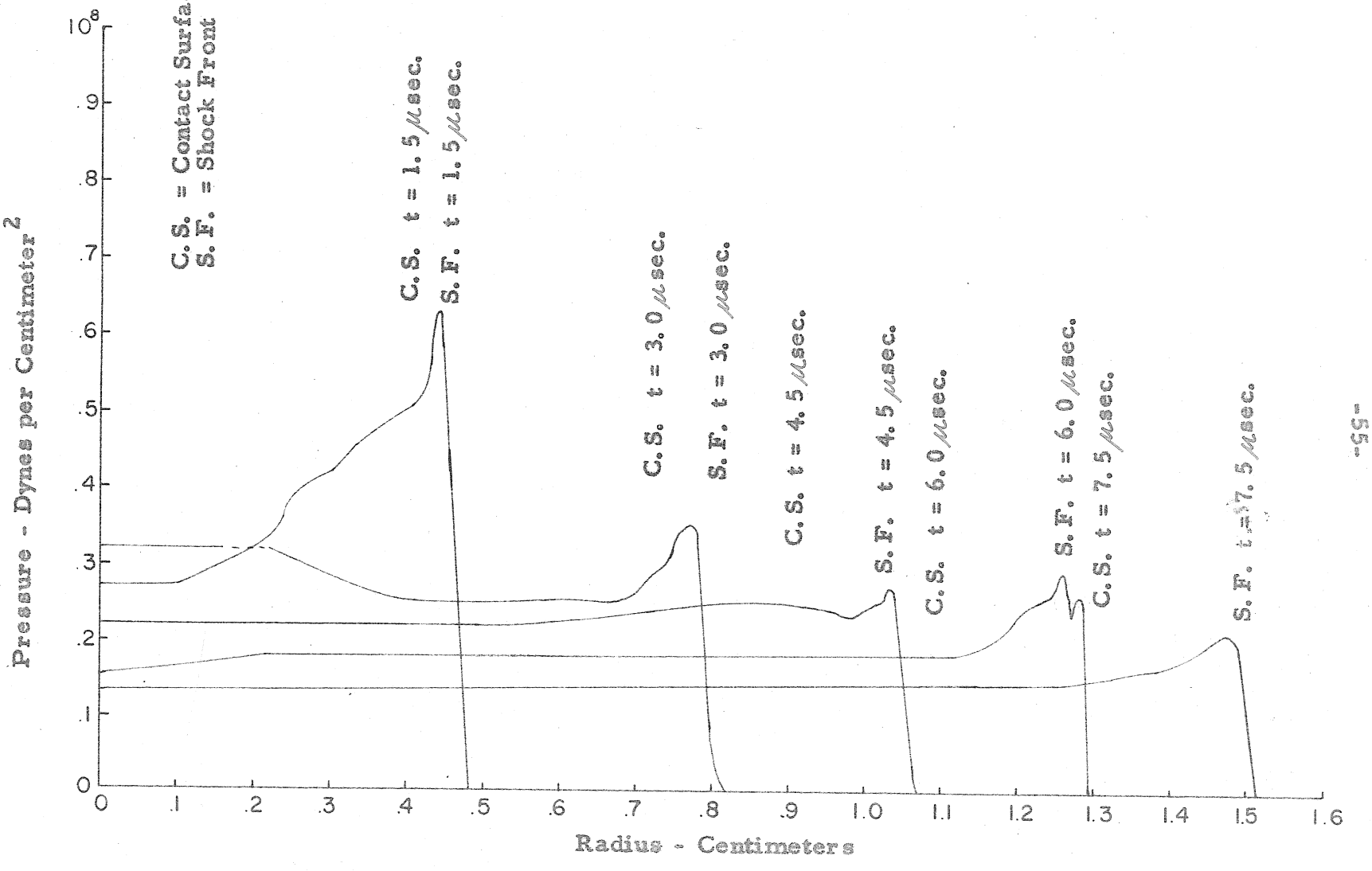

Fig. 39. Pressure profiles at different times from Calculation II

V. EXPLOSION OF WIRES IN VACUUM

Purpose of the Observations

Vacuum explosions have found an application in the production of thin films and may also be usable as a means of producing dense atomic beams, so that it is worthwhile to observe their behavior. In spite of this, very little attention has been given to the electrical explosion of wires in a vacuum as compared with explosions in air and denser media. As far as the author knows, no Kerr cell pictures of the explosion in a vacuum have been reported. Possibly the explanation for this is that many of the spectacular features of the air explosion are absent. There is no shock wave, no current pause, no impressive undulations of the contact surface, and, in fact, a contact surface hardly exists since the surface of the exploded wire becomes very diffuse. However, a study of vacuum explosion is useful because the result in this case should depend more strongly on the properties of the explosion phenomenon itself.

Experimental Procedure

The electrical setup was the same as used for the air explosions and described in part III. The capacitors consisted of the two banks, 7.5 microfarads each, connected in series. This 3.75 microfarad combination was charged to slightly less than 40 kv giving a total stored energy of approximately 3000 joules. The explosion chamber is shown in Fig. 40. At first, fused tungsten to glass seals were used where the electrodes entered the vacuum chamber. However, during the explosion, because of thermal shock or a shock wave traveling

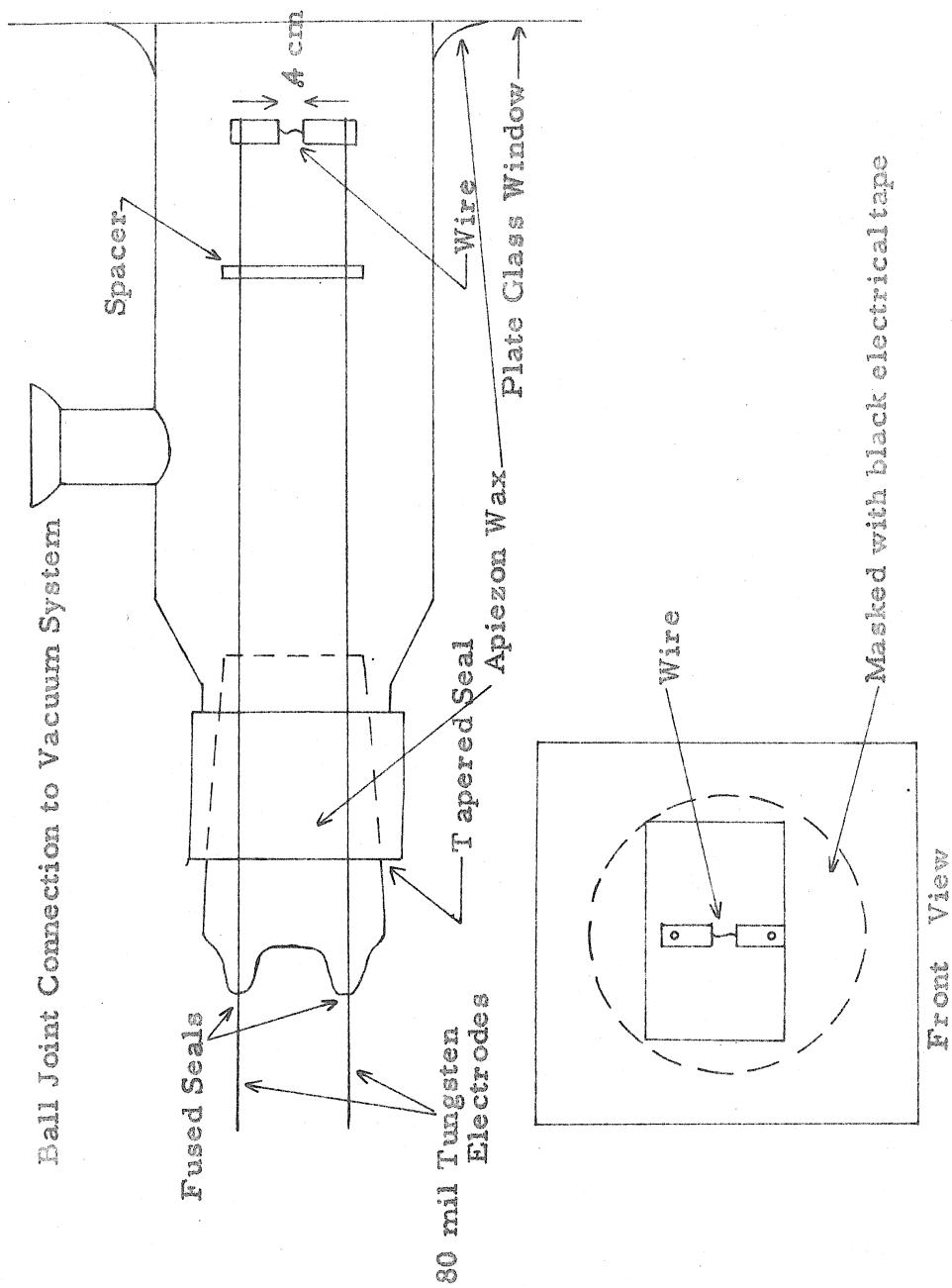

Fig. 40. Vacuum explosion chamber

down the electrodes from the explosion, or perhaps from the strong magnetic force repelling the two electrodes, the seal would often crack. For this reason, the whole base of the explosion chamber was filled with apiezon wax which formed a reliable seal for the electrodes. The plate glass front of the chamber, which became so badly pitted that it had to be replaced after a few explosions, was also attached with this wax. All of the window except for a slit showing the wire was masked with black electrical tape to prevent reflection of light from the inside surface of the chamber.

The spark breakdown voltage of air is such that vacuums of at least one-half mm Hg must be attained to avoid air conduction. However, this is not a sufficient vacuum for the motion of the explosion products to be unaffected by the presence of air. The results presented here were obtained with vacuums of approximately 10^{-5} mm Hg. No noticeable difference was detected when the chamber was evacuated to 10^{-6} mm Hg. The vacuum was measured with a Phillips gauge which had been previously calibrated against a McLeod gauge.

Observations

The pictures shown in Figs. 43 through 52 show much the same behavior for different types of wires. In these pictures, there were $2\frac{1}{2}$ microseconds between frames and the length of the wire was 4 mm. All boundaries were quite diffuse as would be expected of explosions in a vacuum. A very interesting feature of these explosions was that in a matter of about 5 microseconds a configuration with a luminous disk, such as that pointed out by the arrows in Fig. 43, was formed between

the electrodes. A similar configuration had been observed in arcs and sparks by Maecker and Haynes[19, 20], using atmospheric pressure and currents of a few hundred amperes. However, in the pictures presented here, the disk was much more pronounced, sometimes appearing as a thin line between the electrodes, and the completely new feature of the curvature of the disk was present, excellent examples of which were the 2 mil and 3.95 mil diameter iron. The curvature is toward the negative electrode.

Because of the similar appearance of the photographs, it was thought that possibly what was being observed was an arc across the electrodes rather than a true wire explosion. To determine whether the luminous material was from the wire being exploded or from the electrodes, a study of the spectral lines was made when an iron wire was exploded between electrodes of pure copper. The resulting spectrum was that of iron.

Small differences between the explosion of various types of wires could be noted. The disks which tungsten forms were comparatively small in extent and curvature. In the case of 2 mil diameter silver wire, the first frame showed evidence that one end of the wire exploded before the other. This also happened in the air explosion of silver in one instance, see Fig. 29. Iron formed large curved disks as shown in Figs. 43 and 45. Figures 48, 49 and 50 show the copper wire expanding outward initially in the shape of a hollow cylinder. This initial behavior was more pronounced with copper than the other metals.

It was not possible to get accurate voltage oscillograms because of the large inductance of the electrodes of the vacuum chamber and

the small voltage drop across the exploding wire itself. Voltage and current oscillograms were recorded with the voltage divider placed across the leads on the outside of the vacuum chamber. The voltage oscillogram turned out as calculated from the inductance involved verifying that there was only a very small voltage drop across the exploded wire. The current oscillogram was the same, independent of the type of wire exploded, since the wire represented a very small perturbation on the circuit. The current oscillogram was obtained using the same resistor as in part III, and the current form is shown in Fig. 42.

Discussion of Results

In the case of arcs and sparks, the luminous disk which formed in the center has been explained by Cann and Maecker[18, 19] quantitatively as a magnetic effect of the explosion current. The explosion process was concluded to proceed roughly as described below. The wire vaporized and began to expand outward as a hot gas. The initial photographs of the copper wire explosions showed this step well. The current entered and left this conducting channel formed by the metal vapor from an extremely small hot point on the wire holder, probably from the tips of the wire which remained unexploded in the jaws of the wire holder. This gave the conduction channel a shape somewhat as shown schematically in Fig. 41(a) which has a much larger cross-section in the middle than at either end. As a first approximation, exact only in the case where $\bar{B}\cdot\nabla\bar{B}$ vanished, it was assumed that

$$p + \frac{B^2}{2\mu_o} = \text{constant}$$

where $\overline{B}$ was the magnetic field, and p was pressure in the exploded wire vapor in mks units. This approximation stated that $B^2/2\mu_o$ may be regarded as a magnetic pressure and the sum of magnetic and material pressure was constant. When the material pressure was plotted for various cross-sections of the conduction channel, the result was as indicated in Fig. 41(b), the exact shape of the pressure profiles depending on the current distribution. This showed that an overpressure along the axis of the conduction channel existed, the magnitude of which depended on the cross-section of the channel, and so gave rise to a pressure gradient along the axis of the channel. This caused the material to accelerate toward the larger cross-section from both ends. When these "plasma jets" collided in the center, the disk was formed as shown in Fig. 41(c).

The magnitude of the material velocity in the axial direction was related to the cross-sectional area increase by G. Cann[18] in mks units as follows:

$$u = u_o + \frac{\mu_o I^2}{8\pi \dot{m}} \ln \frac{A}{A_o}$$

where A was the cross-sectional area, u was the velocity of the material in the axial direction, I was the current flowing through the exploded wire, μ_o was the permeability, $\dot{m}$ was a constant in this case and equal to ρuA where ρ was the density. Also to be presented and discussed in Reference 18 will be an equation determining the area change from the amount of the energy added to the gas.

An estimate of the velocities, u , from the above equation using $\rho A = 2 \times 10^{-5}$ kg/m , $I^2 = 10^9$ amp, and $\log A/A_o = 4$ gave a value of

3×10^3 m/sec. Along with the above velocity, there was also a drift velocity of both the ions and the electrons caused by the electric field which introduced an asymmetry between the plasma stream that came from the positive side of the wire holder and the one that came from the negative side. Another possible cause of an asymmetry was that the initial cross-section of the channel might have differed from uneven explosion. If some asymmetry caused a difference in momentum carried by the two streams which met in the center, then instead of forming a flat disk, the material from the stream with the greatest momentum would have spilled over the disk and caused the disk curvature. This disk curvature was a new phenomenon which has not been reported in arcs and sparks so far as the author knows. A complete understanding of it should give new insight into the vacuum explosion of wires.

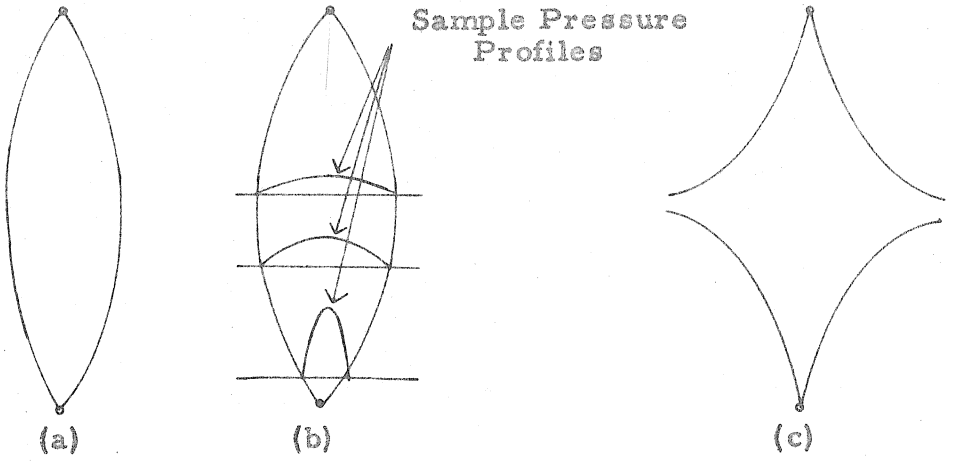

Fig. 41. Formation of disk during vacuum explosions

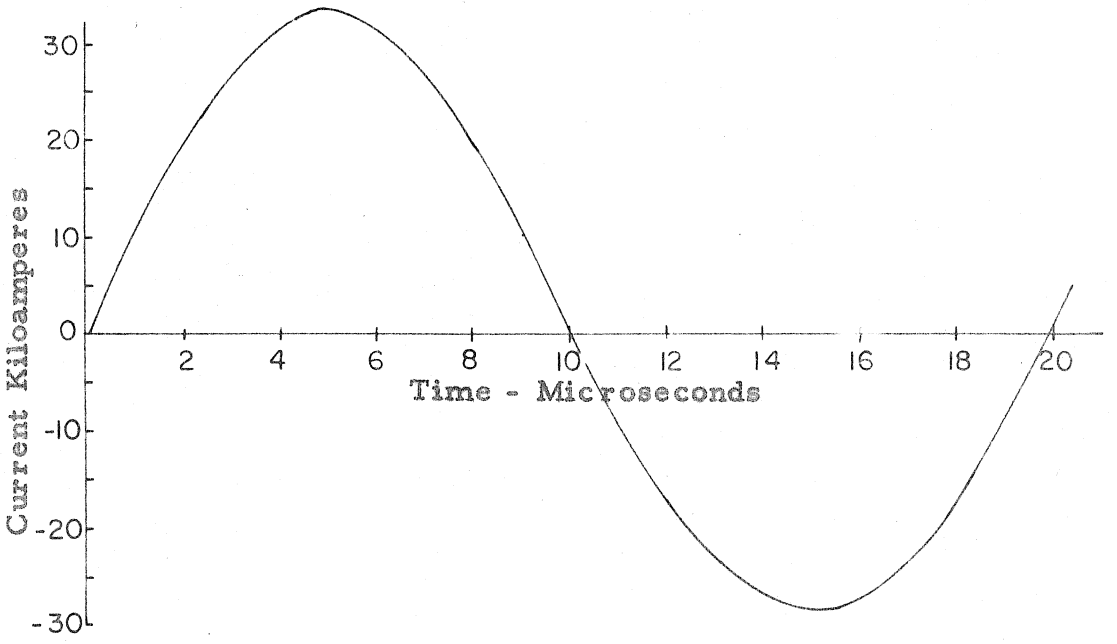

Fig. 42. Current shape during vacuum explosions

Fig. 43. Kerr cell photograph of 3.95 mil diameter iron wire in vacuum

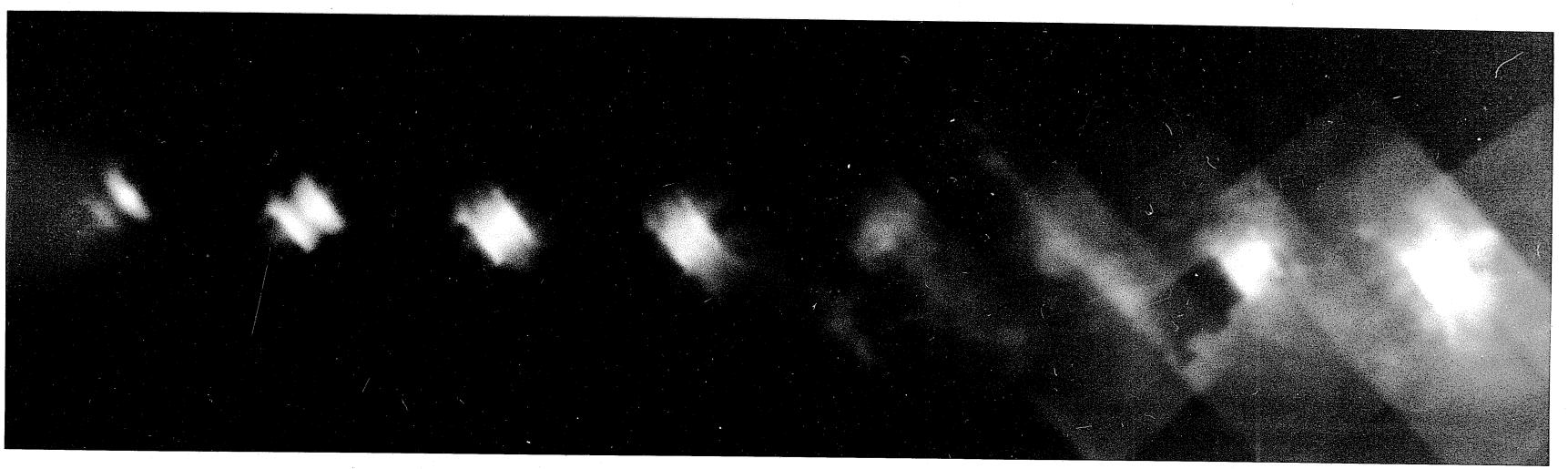

Fig. 44. Kerr cell photograph of 3.0 mil diameter iron wire in vacuum

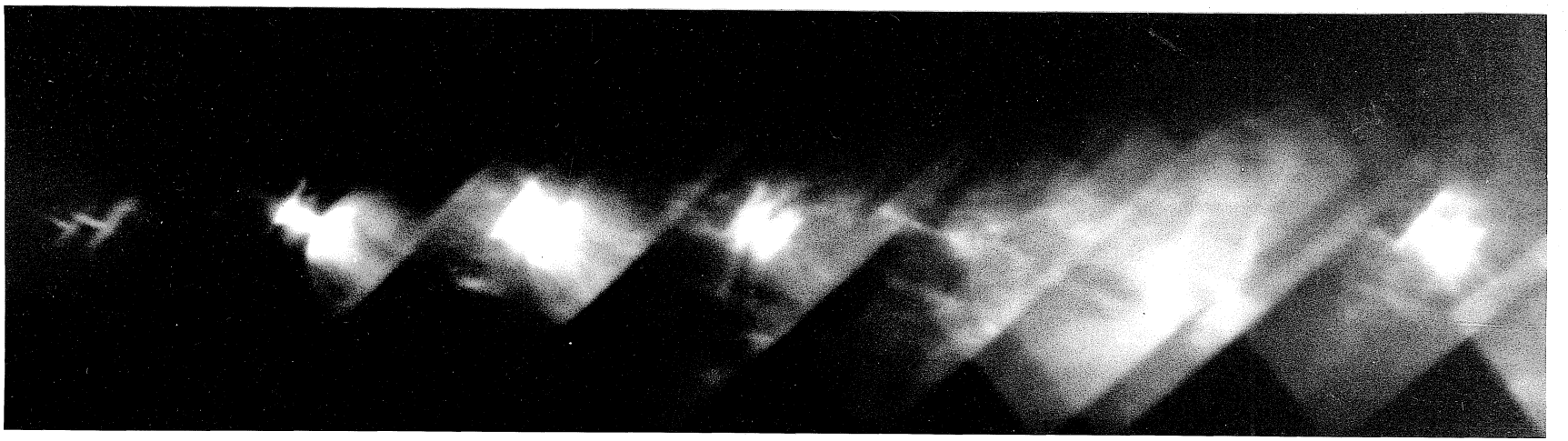

Fig. 45. Kerr cell photograph of 2.0 mil diameter iron wire in vacuum

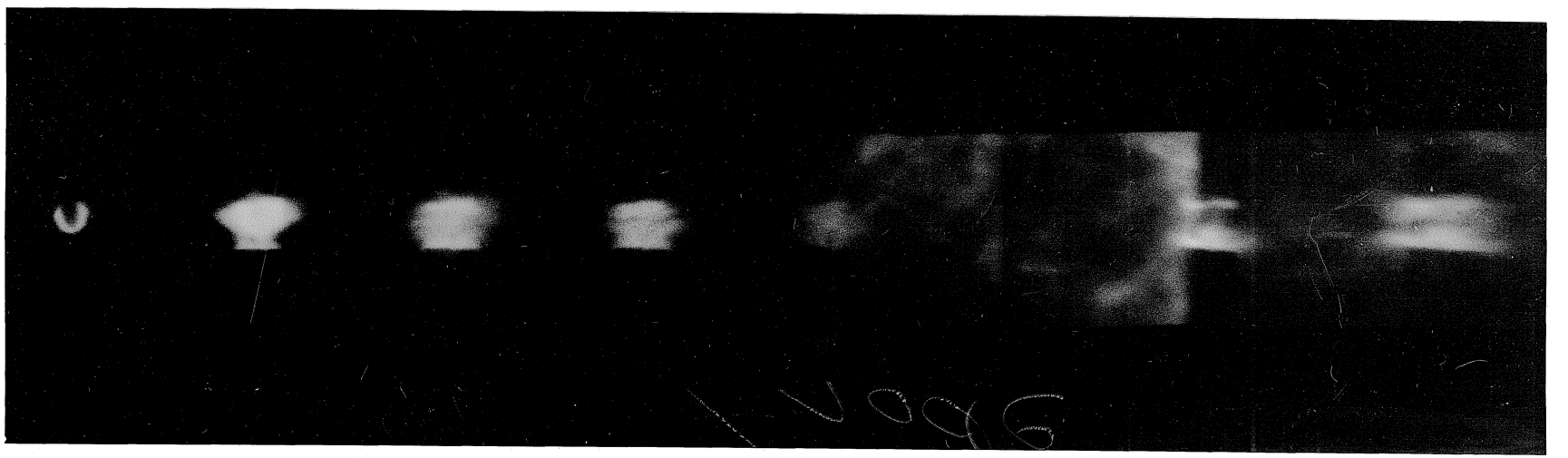

Fig. 46. Kerr cell photograph of 2.0 mil diameter silver wire in vacuum

Fig. 47. Kerr cell photograph of 1.0 mil diameter silver wire in vacuum

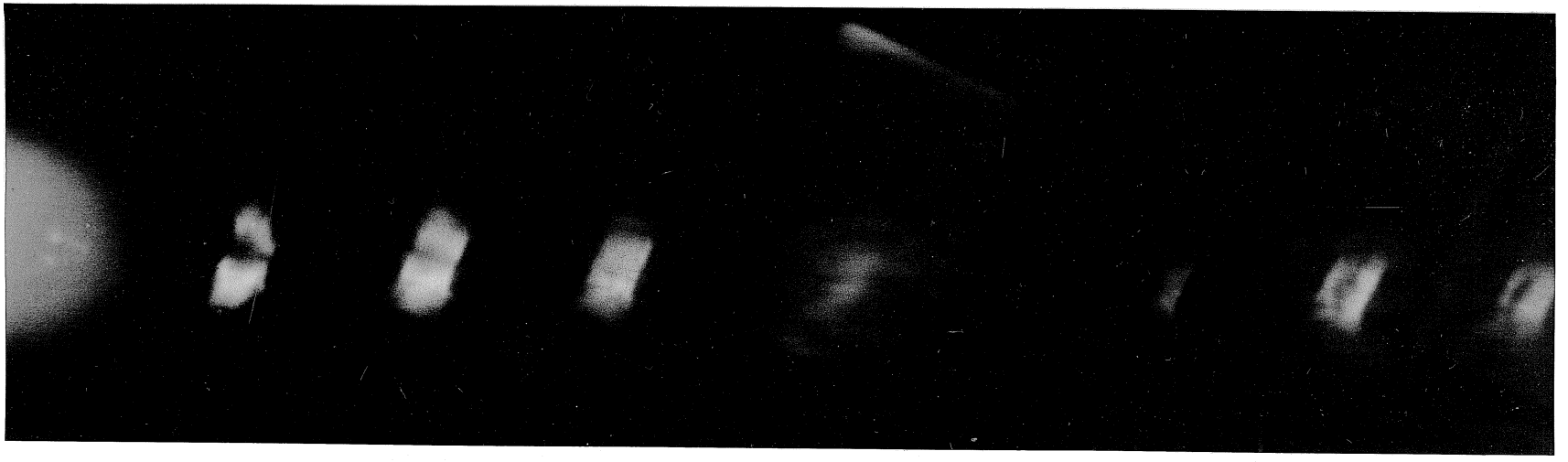

Fig. 48. Kerr cell photograph of 3.15 mil diameter copper wire in vacuum

Fig. 49. Kerr cell photograph of 2.0 mil diameter copper wire in vacuum

Fig. 50. Kerr cell photograph of 1.0 mil diameter copper wire in vacuum

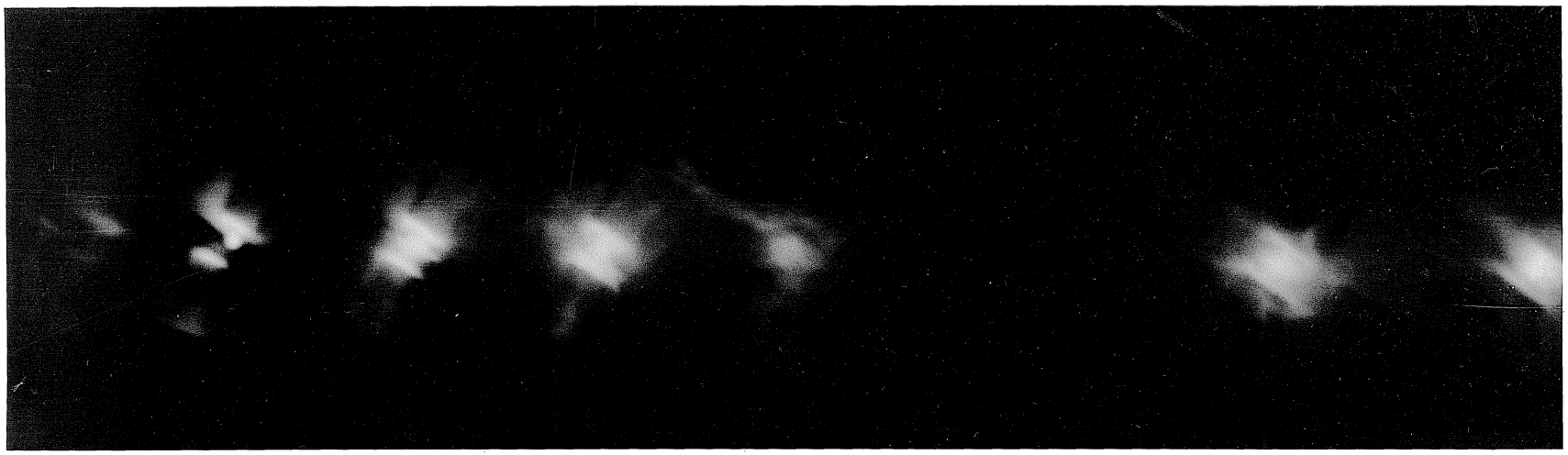

Fig. 51. Kerr cell photograph of 2.0 mil diameter tungsten wire in vacuum

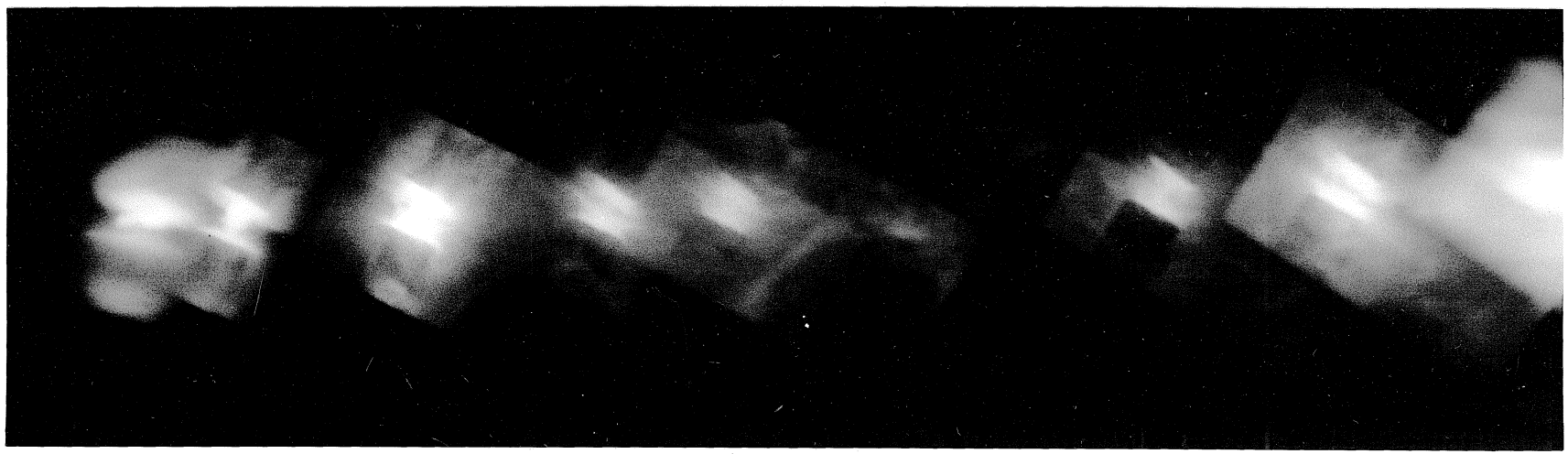

Fig. 52. Kerr cell photograph of .5 mil diameter tungsten wire in vacuum

VI. DETERMINATION OF TIME INTEGRATED CONTINUOUS SPECTRA OF EXPLODING WIRES

Purpose

An accurate experimental determination of the temperature of an exploding wire, in principle, could have been done spectroscopically by a study of line broadening or by utilizing known relative f-values. The first method would have had to rely on theories of broadening which were not generally accepted. The second method could have been used, although there remained much work to be done before these relative f-values would be accurately known for all elements. If the continuous spectra of an exploding wire were to have had a blackbody distribution, this would have provided the best possible determination of temperature and would have been a very important result. Since a time-integrated radiation measurement was used, the current was made to be as nearly a square wave as possible. The power input into the wire was then even more uniform with time than the current except right at the beginning of the explosion when the resistance was relatively high. Figure 17 shows the shape of the measured power input which was kept constant for approximately 25 microseconds.

Regardless, however, of the shape of the spectral energy distribution, its determination was certainly worthwhile as a basis for possible future theoretical work. Furthermore, one of the many applications of an exploding wire is its use as a light source, and very often it is important to know roughly the relative spectral energy distribution of light sources used.

Discussion of Continuous Radiation of Gases

A brief discussion of the conditions necessary for blackbody radiation as presented by Finkelnburg[13] and the application to exploding wires is given here. Using Kirchoff's law and an expression for the absorbed fraction of incident radiation as it passes through an absorbing layer, the spectral emissive power for any radiator can be written as

$$J(\lambda, T, d, n, a) = \left[1 - R(\lambda, T)\right] \left[1 - e^{-a(\lambda, T)d}\right] J_s(\lambda, T)$$

where

$J(\lambda, T, d, n, a)$ is the spectral emissive power of the radiator,

λ is the wavelength,

T is the temperature

d is the thickness of the radiator,

$a(\lambda, T)$ is the absorption coefficient

$R(\lambda, T)$ is the surface reflectivity which can be computed using the Fresnel formula,

$J_s(\lambda, T)$ is the spectral emissive power of an ideal blackbody.

In the special case of emission of hot gases, the reflectivity is very nearly zero because the refractive index, n, is nearly one and the extinction coefficient is almost zero except at resonance lines, which are insignificant[13] when the total radiation is considered. Thus the emission formula becomes

$$J(\lambda, T, d, a) = \left(1 - e^{-a(\lambda, T)d}\right) J_s(\lambda, T)$$

Since the absorption coefficient, a, is always different from zero because of the many free electrons for a very hot gas, this formula

shows the interesting result that the gas would emit blackbody radiation, provided that the radiating layer were thick enough.

The above formula is useful regardless of the form of spectral energy density of the exploding wire because the absorption coefficient should be computable from various atomic constants, the data presented in Part IV of this study, and the equation of state of copper given by Rouse[11]. It would be interesting, but perhaps very difficult, to try to reproduce the spectral energy density of exploding wires using this data.

Experimental Procedure

In obtaining the spectral energy density of the exploding wire under known conditions, the spectroscopic plates containing the spectrum of the exploded wire had to be calibrated and standardized. There were many ways in which the plate could be calibrated, each having its own requirements for use; the choice of a particular one depended upon its convenience and the accuracy required. The method chosen was the step slit using a steady auxiliary source and multiple-exposures. This method required a continuous spectrum, and care had to be taken to avoid diffraction errors and the Eberhard effect. The slit widths used were .67 cm, .46 cm, .30 cm, .20 cm, .145 cm, .095 cm, .07 cm, .05 cm, and .035 cm. To time the exposure on the step slit a Wollensak shutter with 1/10 second exposure was used.

Because multiple exposures were used, it was necessary to insure that the variation in the time that the Wollensak shutter remained open was small enough to be acceptable. This was checked using a

photocell and Berkeley counter arrangement. When the shutter opened light fell on the photocell which gave a signal causing the counter to start and a similar signal stopped the counter. It was found that the R. M. S. deviation from the mean exposure was .6 per cent at 1/10 second exposure. For longer exposures the per cent R. M. S. deviation was less; for shorter ones, more. The criterion given by Sawyer[14] is that the timing must remain accurate to 1 per cent or better. Therefore, this shutter was satisfactory for exposures of 1/10 second or longer.

In general, to avoid errors due to failure of the reciprocity law, the calibration marks should have the same exposure time as the spectrum being investigated. In this case, because of the short time involved with the exploding wire, this was impractical unless other exploding wires had been used, which would have presented problems because their radiation was so very intense and the reciprocity problem would still have remained in the standardization of the plates. Reciprocity effects are usually studied by measuring the amount of exposure, the product of intensity and time, required to obtain a constant density at different intensity levels. Figure 54 is an example of such a curve, and shows the reciprocity effect for Kodak 50 plates, which were used in this research. If the reciprocity failure curve were completely independent of factors such as wavelength of the exposing radiation and density produced on the plate, then it would have no effect at all in the final result of relative spectral energy density for the exploding wire. The density produced by the exploding wire would have been altered throughout the whole wavelength interval studied relative to the densities produced by the calibration marks, but the net

effect would have been the same as if the calibration marks had been impressed with a slightly different exposure time.

This left two ways that the reciprocity law failure might have affected the result obtained here; (1) the variation of reciprocity failure with wavelength, and (2) its variation with density. The first of these was not serious because, according to information furnished by Kodak on their spectroscopic plates, reciprocity characteristics were nearly independent of the spectral quality of the exposing radiation when points of the same density were considered. Examining this point further showed that if the reciprocity failure curves for a given material and development conditions were plotted so that the logarithm of exposure time, t, was the abscissa and the logarithm of exposure, I_t, was the ordinate, the curves for different wavelengths were displaced vertically from one another but had the same shapes as shown in Fig. 55. From this figure it was evident that if, as different wavelengths were considered, the exposure of the calibration marks had to be increased by some factor to produce a given effect with exposure time t_2, then the exposure of the exploding wire with exposure time t_1 was increased by the same factor to produce the same effect as if there were no variation with wavelength. This type of variation with wavelength produces no effect, just as differences in the dispersion of the spectrograph do not matter, in the final result for the relative spectral energy density of the exploding wires.

The importance of the variation of the reciprocity law failure characteristics with density for this problem was not quite so easily determined. The question was this: did comparing one line of constant

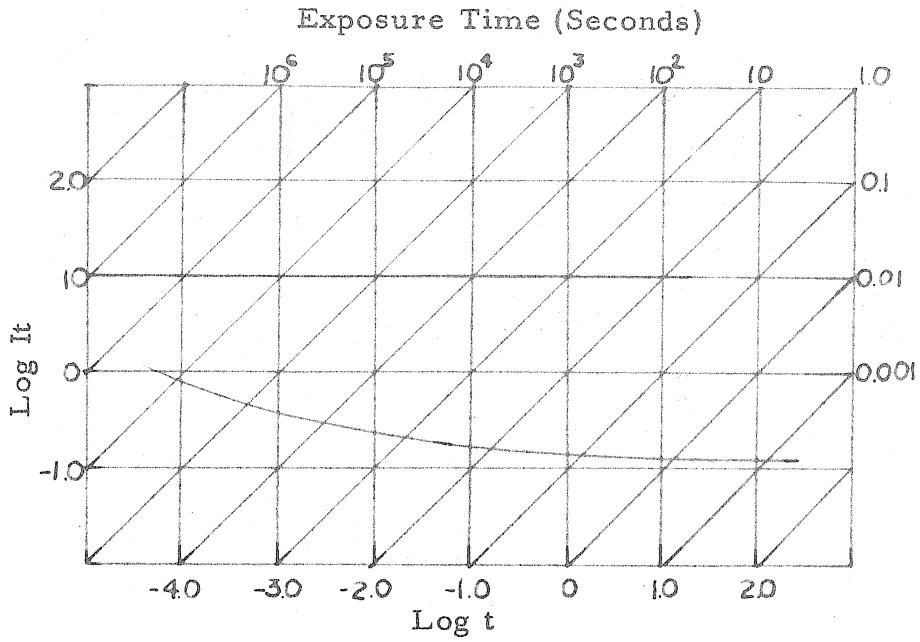

Fig. 53. Reciprocity characteristic of Kodak 50 plates

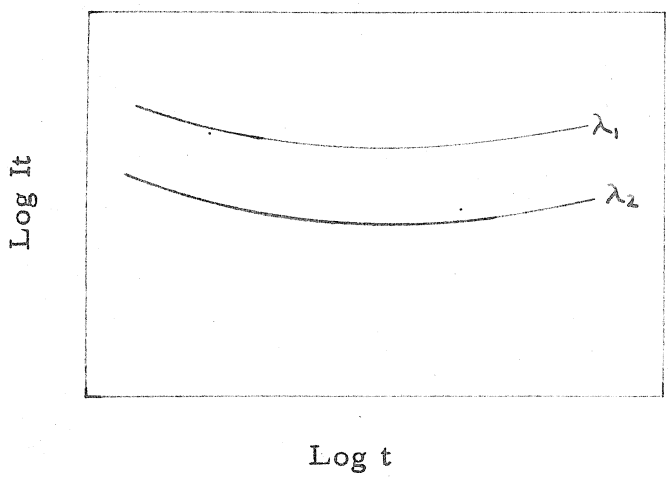

Fig. 54. Sample reciprocity characteristic of light of different wave lengths

density to another involve the same ratio of intensities at an exposure time corresponding to the exploding wire as when the exposure time was that of the calibrating and standardizing lamp? Experimental evidence, published by Arens and Eggert[14], and shown in Fig. 56, indicated this to be approximately the case. The conclusion was then, that in finding relative spectral energy distributions, reciprocity law failure had only a minor effect on the final result. A thorough discussion of reciprocity is given by Mees[15].

Temperatures expected in the exploding wire in air were in excess of 10,000°K [2]. This temperature region plus the available spectrograph, a Hilger medium quartz, suggested the wavelength interval of from 2300 Å to 5500 Å for this study. Other considerations involved in the choice of a calibrating and standardizing lamp were:

1. The radiation should be as nearly uniform from 2300 Å to 5500 Å as possible;

2. The lamp should yield an irradiation that is as constant with time as possible;

3. The lamp should have a reasonable purchase price.

After an investigation, it appeared that a Beckman No. 8333 hydrogen lamp would most nearly meet the requirements. This lamp was specially made for use in the Beckman spectrophotometer for which requirements 1, 2, and 3 are also applicable.

The relative spectral energy density of this lamp was determined using a Beckman model DU spectrophotometer which gave the response of a 1P28 photocell for different wave lengths when the No. 8333 hydrogen discharge lamp was used as the spectrophotometer light source.

In this case, as when the lamp was used with the spectrograph, the lamp was placed about four feet from the entrance slit and the light from the central blue spot was focused on the slit with a 5 cm focal length quartz lens placed near the lamp so that only the central portion of the image passed through the slit.

To obtain the relative spectral energy of the lamp, the photocell response was corrected for the spectral sensitivity characteristic of the 1P28 photocell, the spectral reflectivity of the aluminized surfaces, and the varying dispersion of the quartz prism over this wavelength region. The S-5 response of the 1P28 was obtained from RCA and was said to be accurate to $\pm$ 15 per cent. According to the spectrophotometer instruction manual, the photocells used were selected, so perhaps this figure was high. The spectral reflectivity of aluminum was obtained from Reference 17 and the dispersion was given in the spectrophotometer instruction manual. These spectral characteristics along with the uncorrected photocell readings are shown in Fig. 57. Figure 58 gives the resulting relative spectral energy distribution of the Beckman No. 8333 hydrogen lamp under the conditions described.

In exposing the spectrograms, first a wavelength scale was impressed, then the exploding wire spectrum (using stops to keep from overexposing), and finally the calibration marks were impressed. Kodak 50 plates were used and developed in D-19 developer. The recording microphotometer described in part II was used to analyze these plates.

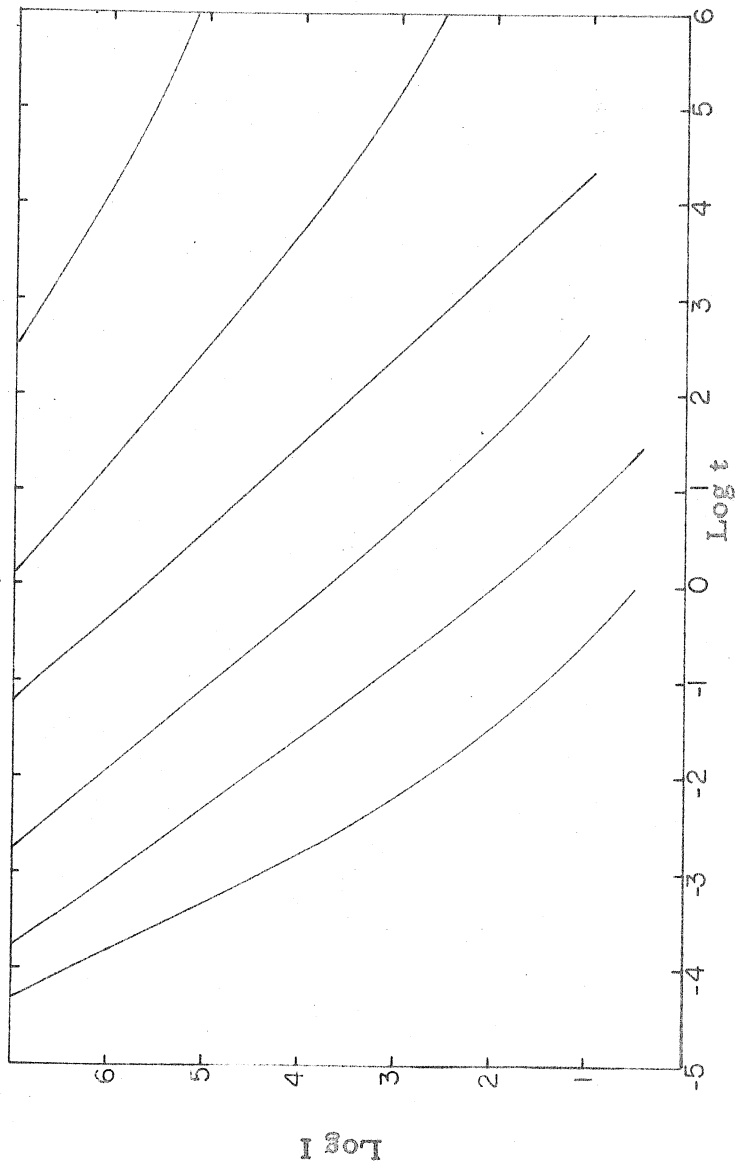

Fig. 55. Lines of constant density in a log I versus log t diagram

Results

From this data, Fig. 58 was obtained, which gives the resulting relative spectral energy density of the 3 mil diameter iron wire. Wires were exploded with the storage condensers, total capacity 24 microfarads, charged to three different voltages, 5 kv, 10 kv, and 15 kv. Note that points on each curve give a value relative only to points on the same curve; no relationship was obtained between points lying on different curves. The higher initial voltage cases gave off considerably more light and required more stopping down in the optics of the spectrograph. See Fig. 17 for the power input to the wires. This was obtained in the manner discussed in part III.

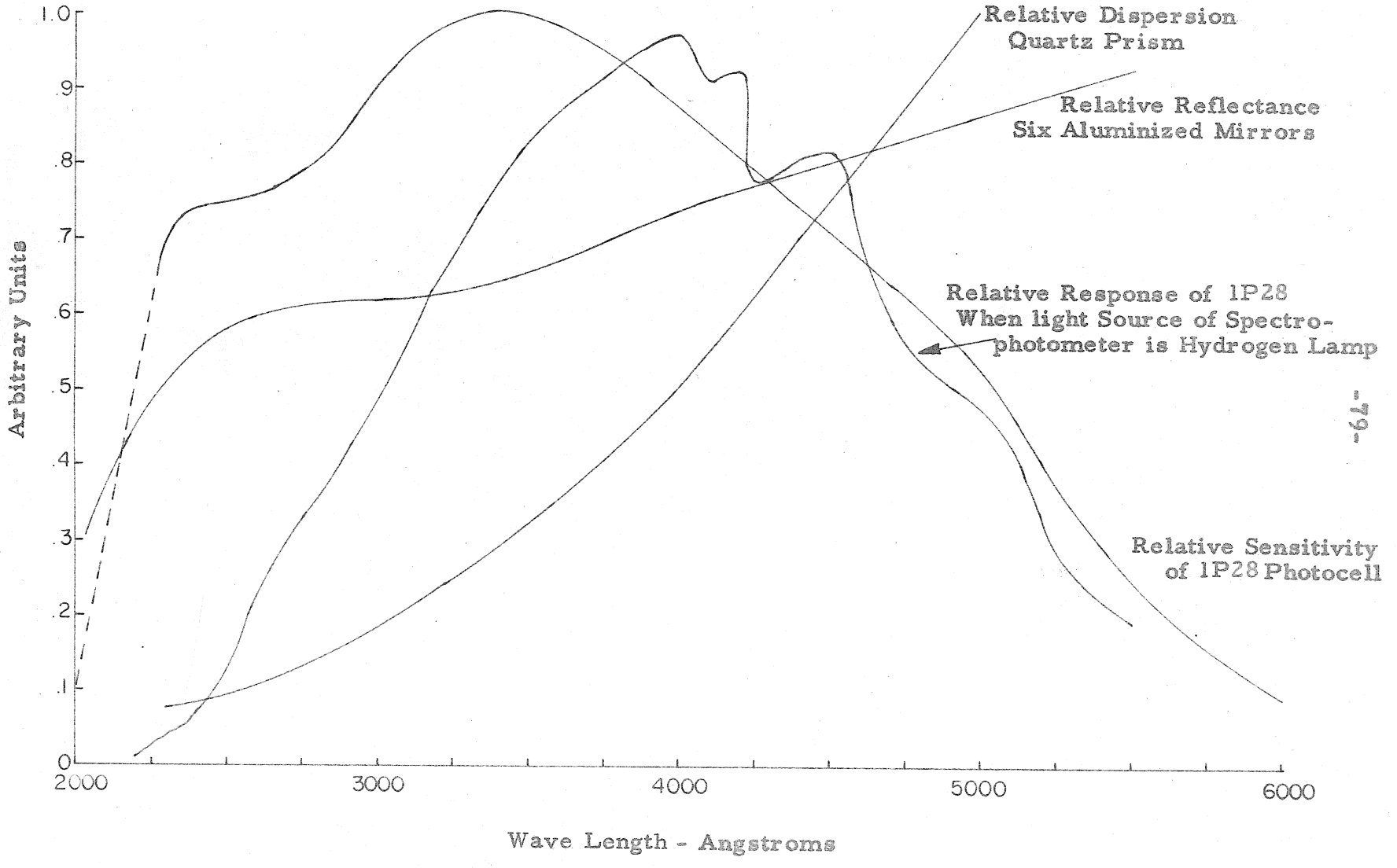

Fig. 56. Relative spectral dependences

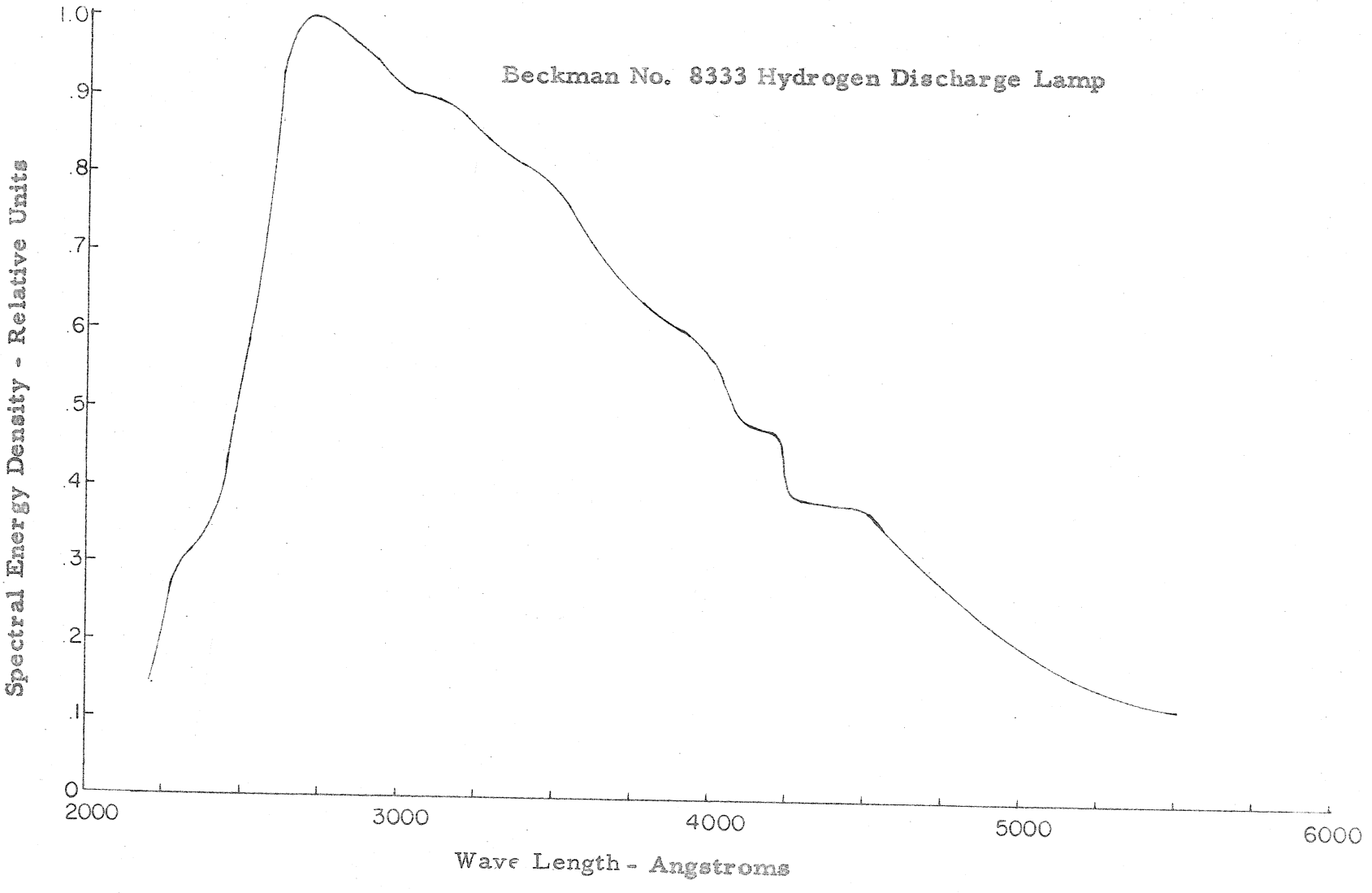

Fig. 57. Spectral energy density of Beckman No. 8333 lamp

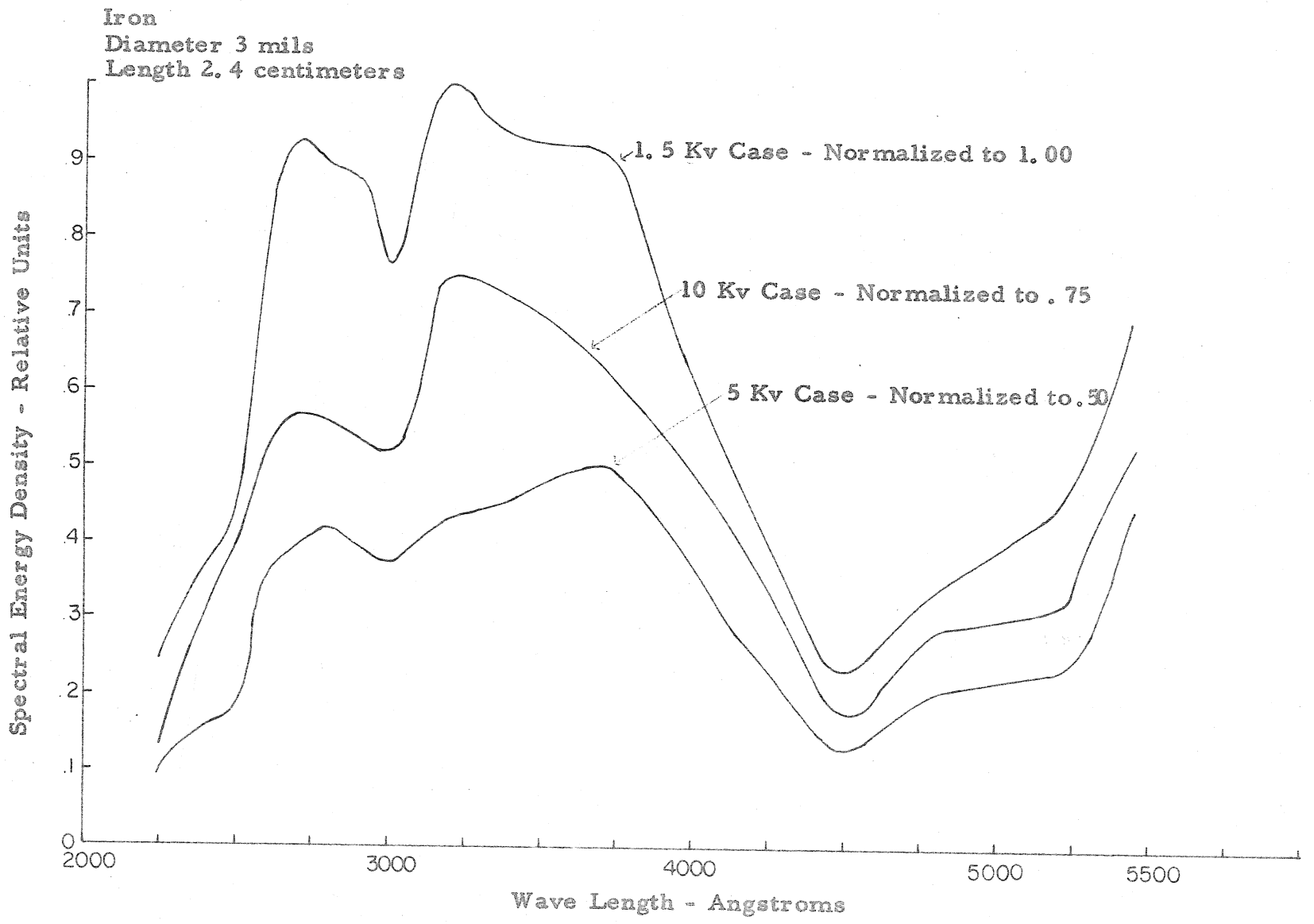

Fig. 58. Relative spectral energy density of exploded iron wire

VII. SUMMARY

Observations were made of wire explosions in air using a Kerr cell camera capable of repetitive photographs. The frames were $2\frac{1}{2}$ microseconds apart. Simultaneous electrical measurements of the voltage and current of the wire were made. The results were presented in graphical form with each graph showing the position of the shock front, the position of the contact surface, and the instantaneous power into the wire as functions of time up to approximately 7 microseconds. The data was obtained for wires of iron, copper, silver, tungsten, and aluminum of various diameters ranging from $\frac{1}{2}$ mil to 4 mils. Also presented, in order to illustrate the behavior of the wires, are examples of the resulting photographs.

In the case of the 3.15 mil diameter copper wire, calculations were carried out with an IBM 704 Lagrangian code. The model used was the same as reported by Rouse[6] except that a source term was added to the energy equation. The equations of state for the copper and surrounding air were obtained from a solution of Saha's equation.[11, 12] The results concerning the hydrodynamic flow are presented in the same manner as used for the experimental data so that the theoretical results may be compared with the experiments. Pressure, density, and velocity profiles from the calculations are included.

The explosion of wires in a vacuum was studied using the Kerr cell camera, and the interesting phenomenon of the formation of a curved luminous disk between the electrodes was observed. This disk was similar in appearance to those reported in arcs and sparks[19, 20] except for the curvature which, as far as the author knows, has not

been previously reported in arcs, sparks, or exploding wires. An explanation for the formation of this disk is given. A further investigation of this phenomenon might be rewarding, since the curvature could be accurately measured. Photographs of the explosion of the different wires are presented.

The relative spectral energy density of exploding iron wire was measured using different initial stored energies. This measurement was done using a Hilger medium quartz spectrograph and compared the spectrum obtained with that of a hydrogen discharge lamp which had its relative spectral energy density previously determined by the use of a spectrophotometer. Corrections were made to the spectrophotometer reading to account for the varying dispersion of the instrument, the spectral reflectivity of the mirrors involved, and the spectral sensitivity of the photocell. The latter factor, the spectral response of the photocell, probably accounted for the largest error in this determination of the relative spectral energy density of exploding iron wire. The photographic plates were calibrated using a step slit. The effect of reciprocity law failure on the result was studied and concluded to introduce only a very slight error. From the information obtained from the hydrodynamic flow studied, it should be possible to compute a theoretical relative spectral energy density which could then be compared with the experimental result presented here.

REFERENCES

1. Anderson, J. A., Astrophys. J., 51, pp. 37-48 (1920)

2. Anderson, J. A. and Smith, S., Astrophys. J., 64, pp. 295-314 (1926).

3. Kvarkhtsave, I. F., Pliutto, A. A., Chernov, A. A., and Bondarenko, V. V., Soviet Phys. JETP, 3, pp. 40-51, (1956).

4. Kvartskhave, I. F., Bondarenko, V. V., Meladze, R. D., and Suladze, K. V., Soviet Phys. JETP, 4, pp. 637-644(1957).

5. Lin, S. C., J. of App. Phys., 25, p. 54 (1954).

6. Chace, W. G. and Moore, H. K., eds., Exploding Wires, Plenum Press, New York (1959).

7. Proceedings of a Symposium held at the National Physical Laboratory on Sept. 14-17, Cavitation in Hydrodynamics, Philosophical Library, Inc., New York, pp. 1-8, (1955)

8. Bennett, F. D., Phys. of Fluids, 1, pp. 347-352, (1958).

9. Bondarenko, V. V., Hvartskhave, I. F., Pliutto, A. A., and Chernov, A. A., Soviet Phys. JETP, 1, p. 221, (1955).

10. Chace, W. G., Phys. of Fluids, 2, p. 230 (1959).

11. Rouse, C. A., Theoretical Calculations of Exploding Wire Phenomenon, University of California Radiation Laboratory 5684-T, Livermore, California (1959).

12. Gilmore, F. R., Equilibrium Compositions and Thermodynamics Properties of Air to 24,000°K, Rand Corp., RM-1543, Santa Monica, Calif. (1955).

13. Finkelnburg, W., Conditions for Blackbody Radiation by Solids and Gases, Engineer Research and Development Laboratories, Fort Belvoir, Virginia, pp. 1-10 (1948)

14. Arens, H. and Eggert, J., Z. Phys. Chem., 131, p. 297 (1928).

15. Mees, C. E. K., The Theory of the Photographic Process, Mac-Millan, New York, pp. 199-242 (1954).

16. Sawyer, R. A., Experimental Spectroscopy, Prentice-Hall, New York (1946).

17. Allen, C. W., Astrophysical Quantities, University of London, London, p. 102 (1955).

18. Cann, G., Thesis, California Institute of Technology, Pasadena, to be published in 1960.

19. Report of the Internation Symposium on Electrical Discharges in Gases, Martinus Nijhoff, The Hague, Netherlands (1955).

20. Haynes, J. R., Phys. Rev., 73, pp. 891-903, (1948).